

Intrinsic Riemannian Functional Data Analysis for Sparse Longitudinal Observations

Zhenhua Lin^{1*} Lingxuan Shao^{2†} Fang Yao^{2‡}

¹*National University of Singapore* and ²*Peking University*

Abstract

A novel framework is developed to intrinsically analyze sparsely observed Riemannian functional data. It features four innovative components: a frame-independent covariance function, a smooth vector bundle termed *covariance vector bundle*, a parallel transport and a smooth bundle metric on the covariance vector bundle. The introduced intrinsic covariance function links estimation of covariance structure to smoothing problems that involve raw covariance observations derived from sparsely observed Riemannian functional data, while the covariance vector bundle provides a rigorous mathematical foundation for formulating the smoothing problems. The parallel transport and the bundle metric together make it possible to measure fidelity of fit to the covariance function. They also play a critical role in quantifying the quality of estimators for the covariance function. As an illustration, based on the proposed framework, we develop a local linear smoothing estimator for the covariance function, analyze its theoretical properties, and provide numerical demonstration via simulated and real datasets. The intrinsic feature of the framework makes it applicable to not only Euclidean submanifolds but also manifolds without a canonical ambient space.

MSC 2020 subject classifications: primary 62R10; secondary 62R30

Keywords: Intrinsic covariance function, vector bundle, parallel transport, diffusion tensor, smoothing, Fréchet mean.

1 Introduction

Functional data are nowadays commonly encountered in practice and have been extensively studied in the literature; for instance, see the monographs Ramsay and Silverman (2005); Ferraty and Vieu (2006); Hsing and Eubank (2015); Kokoszka and Reimherr (2017), as well as the survey papers Wang et al. (2016) and Aneiros et al. (2019), for a comprehensive treatment on functional data analysis. These classic endeavors study functional data of which functions are real- or vector-valued, and thus are challenged by data of functions that do not take values in a vector space. Such data emerge recently, partially due to the rapid development of modern technologies. For example, in the longitudinal study of diffusion tensors, as the tensor measured at a time point is represented by a 3×3 symmetric positive-definite matrix (SPD), the study results in a collection of SPD-valued functions. The space of SPD matrices is not a vector space, and

*linz@nus.edu.sg. Research is partially supported by NUS startup grant R-155-000-217-133.

†shao-14@pku.edu.cn.

‡fyao@math.pku.edu.cn. Research is partially supported by National Natural Science Foundation of China with a Key grant 11931001 and a General grant 11871080, and the Key Laboratory of Mathematical Economics and Quantitative Finance (Peking University), Ministry of Education.

in particular, the usual Euclidean distance on it suffers from the “swelling effect” which introduces artificial and undesirable inflation of variability in data analysis (Arsigny et al., 2007). Specialized distance functions (Pennec et al., 2006; Dryden et al., 2009) or metrics (Moakher, 2005; Arsigny et al., 2007; Lin, 2019) are required to alleviate or completely eliminate the swelling effect. These metrics turn the space of SPD matrices of a fixed dimension into a nonlinear Riemannian manifold. Data in the form of Riemannian-manifold-valued functions are termed Riemannian functional data and modeled by Riemannian random processes which are random processes taking values in Riemannian manifolds (Lin and Yao, 2019).

In addition to infinite dimensionality, statistical analysis of Riemannian functional data is primarily challenged by lack of vector structure of the Riemannian manifold. Consequently, the aforementioned classic works on functional data, which are geared to Euclidean or vector spaces, do not directly apply to Riemannian functional data. This challenge is also shared by non-functional manifold-valued data analysis, on which there exists vast literature. For example, fundamentals related to the Fréchet mean, a generalization of the mean of random variables or vectors for random elements in a Riemannian manifold, were studied in depth by Bhattacharya and Patrangenaru (2003, 2005); Afsari (2011); Schötz (2019); Pennec (2019), while regression for manifold-valued data were investigated by Pelletier (2006); Shi et al. (2009); Steinke et al. (2010); Fletcher (2013); Hinkle et al. (2014); Cornea et al. (2017), and more broadly, for metric-space valued data by Hein (2009); Faraway (2014); Petersen and Müller (2019); Lin and Müller (2019), among many others.

In contrast, the literature on Riemannian functional data is scarce and emerges only in recent years. Su et al. (2014) first represented each trajectory by its normalized velocity curve (called square-root vector field) and then transported the velocity vectors into a common tangent space. While Zhang et al. (2018) specifically considered spherical trajectories and developed a data transformation geared to the spherical geometry, Dai and Müller (2018) studied trajectories on a more general manifold but required the manifold to sit in a Euclidean ambient space. Lin and Yao (2019) developed an intrinsic framework for Riemannian functional data that eliminates the need of an ambient space. Dubey and Müller (2020) investigated metric-space-valued functional data via the device of metric covariance, where each function takes values in a general metric space that includes the Riemannian manifold as a special case. All of these works assume fully observed functional data. The development by Dai et al. (2020) targets discretely and noisily recorded Riemannian functional data, but again requires a Euclidean ambient space.

The mean and covariance functions are two of the most fundamental concepts in functional data analysis, as many downstream analysis depends on them. Therefore, it is of particular importance to generalize them to Riemannian functional data. For the mean function, the generalized counterpart is the well established Fréchet mean function that is adopted in Dai and Müller (2018); Dai et al. (2020); Lin and Yao (2019) as well as this paper. The real difficulty comes from modeling the covariance structure. To tackle nonlinearity of the Riemannian manifold, a strategy commonly employed in the aforementioned works is to transform data from the manifold into tangent spaces via Riemannian logarithmic maps, and then to model the covariance via the transformed data. Specifically, at each time point, the associated observations are transformed into the tangent space at the Fréchet mean in that time point. Although tangent spaces of a manifold are linear spaces and thus provide the desired vector structure, there is one issue to resolve: *Different tangent spaces are distinct vector spaces and thus their tangent vectors are incomparable, but the covariance involves random tangent vectors from different tangent spaces.* More specifically, the value of the covariance function at a pair (s, t) of time points involves observations at both s and t , and in the manifold setting, the observations at these time points are often transformed into tangent vectors of distinct tangent spaces; see Figure 1.

One approach to overcome the above issue, referred to as the ambient approach in this paper, is to place the tangent spaces in a larger common vector space. This approach, adopted in Dai and Müller (2018); Dai et al. (2020), is particularly useful when the manifold comes with a natural Euclidean ambient space,

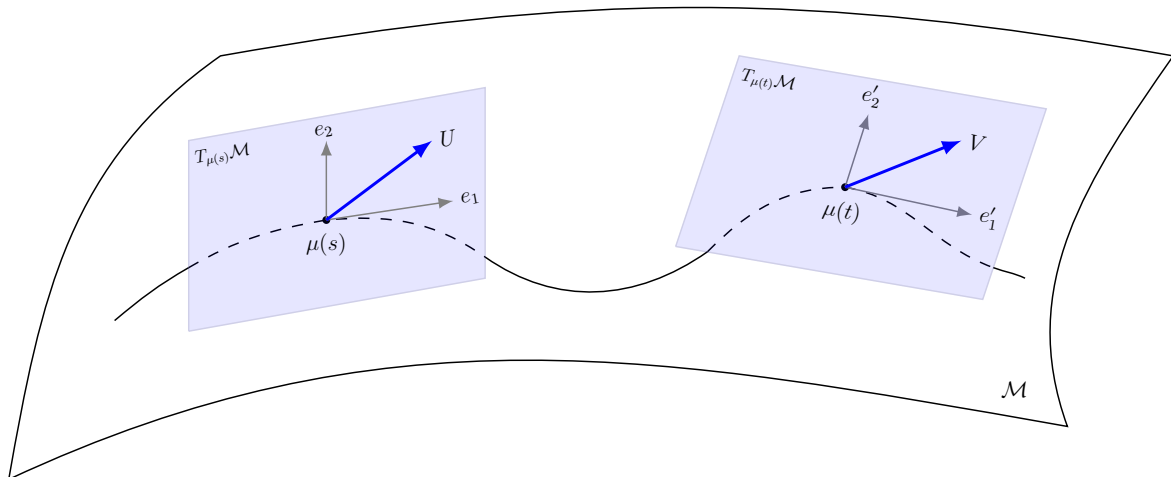


Figure 1: Illustration of random tangent vectors in different tangent spaces. The curve across the manifold \mathcal{M} represents the Fréchet mean function μ defined in (1). The two parallelograms represent the tangent spaces at $\mu(s)$ and $\mu(t)$, respectively. An (random) observation associated with the time s is often transformed into the tangent space $T_{\mu(s)}\mathcal{M}$ at $\mu(s)$; the transformed observation is represented by the tangent vector U in the figure. Similarly, the tangent vector V in the tangent space $T_{\mu(t)}\mathcal{M}$ at $\mu(t)$ represents a transformed observation associated with the time point t . The tangent vectors U and V are incomparable, since they reside in distinct tangent spaces. The vectors e_1 and e_2 represent an orthonormal basis in $T_{\mu(s)}\mathcal{M}$ while e'_1 and e'_2 form an orthonormal basis of $T_{\mu(t)}\mathcal{M}$. The tangent vectors U and V can be respectively represented by their (random) coefficients with reference to the bases $\{e_1, e_2\}$ and $\{e'_1, e'_2\}$. The coefficients are real-valued random vectors and directly comparable, e.g., their covariance can be defined in the usual way.

as the ambient space serves as the common space for the transformed data, but is less appropriate when the manifold does not have a canonical Euclidean ambient space. In addition, operation performed in the ambient space may violate the intrinsic geometry of the manifold and produce undesirable consequences. Another approach, adopted by Lin and Yao (2019), takes a completely intrinsic perspective by treating the transformed data as realizations from a random element in a delicately constructed Hilbert space and then modeling the covariance by the covariance operator of the random element. Since the intrinsic strategy does not refer to an ambient space, it does not suffer from the aforementioned shortcomings of the ambient strategy. However, estimation of the covariance operator in Lin and Yao (2019) requires fully or densely observed functional data.

In light of the major advantage of the intrinsic perspective, it is desirable to model and estimate the covariance structure for sparsely observed Riemannian functional data without reference to an ambient space, which turns out to be rather challenging. For sparse functional data, a common strategy that is well established in the Euclidean setting is to smooth the discrete and noisy raw covariance function (Yao et al., 2005; Li and Hsing, 2010; Zhang and Wang, 2016). However, there are fundamental difficulties in extending this seemingly simple strategy to the manifold setting. First, as previously mentioned, the covariance function involves tangent vectors from different tangent spaces, so that an appropriate definition of covariance between two incomparable random tangent vectors is in order. A possible way is to fix an orthonormal basis for each tangent space and represent the random tangent vectors by their coefficients with respect to the corresponding bases; see Figure 1. The bases are collectively referred to as an orthonormal frame. Then the covariance of two random tangent vectors can be defined as the covariance matrix of their coefficients that are real-valued vectors and thus comparable. The resulting covariance function is indeed the covariance function

of the coefficients of the transformed Riemannian random process with respect to the frame, and can be estimated via smoothing the coefficients of the raw covariance functions with respect to the same frame. However, the estimate obtained by this approach is not invariant to the frame, i.e., different frames result in distinct estimates that can not be linked via an affine transformation, because most smoothing methods are not invariant to the frame; see Remark 3.1 for further discussion. Second, for the smoothing strategy to work, the underlying covariance function shall possess certain regularity of smoothness, such as continuity or differentiability. Without reference to an ambient space or a frame, it is rather challenging to define and quantify such regularity. This problem is unique to sparsely observed data; when data are fully observed or sufficiently dense so that each trajectory can be individually recovered, the sample covariance operator serves as an estimate for the covariance structure (Lin and Yao, 2019), which requires no smoothing.

The major contribution of this paper is to develop a novel framework to intrinsically model and estimate the covariance when Riemannian functional data are sparsely and noisily recorded. The framework features four innovative components.

- First, a frame-independent intrinsic covariance function is developed. This is made possible by considering the covariance of two random tangent vectors in different tangent spaces as a linear operator that maps one tangent space into the other. This covariance function does not require reference to a frame and thus is fundamentally different from the covariance function of coefficients with respect to a frame in Lin and Yao (2019).
- Second, to extend the idea of smoothing a raw covariance function (Yao et al., 2005) to the manifold setting, we construct a novel smooth vector bundle from the manifold, termed *covariance vector bundle*, to provide an appropriate mathematical foundation for intrinsic quantification of the regularity of the proposed covariance function, such as continuity, differentiability and smoothness. For example, it makes statements like “find a *smooth* covariance function that minimizes the mean squared error” sensible. In addition, covariance function estimation is amount to smoothing data located in a smooth vector bundle. Although there is a rich literature on smoothing Riemannian manifold-valued data, the study on smoothing data in a vector bundle is still in its infancy.
- Third, a parallel transport on the covariance vector bundle is developed from the intrinsic geometry of the manifold, which also induces a covariant derivative on the bundle. The covariant derivative allows intrinsic definition of derivatives of a function taking values in the covariance vector bundle. Such derivatives are often needed when one analyzes theoretical properties of a smoothing procedure. The parallel transport also enables one to move the raw observations into a common vector space in which classic smoothing methods apply.
- Fourth, a smooth bundle metric is constructed and plays an essential role in measuring the fidelity of fit to data during estimation and quantifying the quality of an estimator. It is derived from the intrinsic geometry of the underlying Riemannian manifold and utilizes the Hilbert–Schmidt inner product of linear operators between two potentially different Hilbert spaces. Such inner product, mathematically well established (e.g., Definition 2.3.3 and Proposition B.0.7 by Prévôt and Röckner, 2007), is less seen in statistics; the common one is defined for operators that map a Hilbert space into itself.

The frame-independent covariance function and the covariance vector bundle together pave the way for intrinsically smoothing the observed raw covariance function, while the parallel transport and the bundle metric are critical for developing an estimation procedure for sparsely observed Riemannian functional data. As an illustration, we propose an estimator for the covariance function based on local linear smoothing and establish the point-wise and uniform convergence rates of the estimator, while emphasize that other

smoothing techniques such as spline smoothing are also applicable. Other contributions include extending the invariance principle of Lin and Yao (2019) to the sparse design and connecting holonomy theory to statistics via Lemma 4.1 that might be of independent interest.

The rest of the paper is organized as follows. In Section 2, we construct the covariance vector bundle, a parallel transport and a smooth metric on the bundle. In addition, we formulate the intrinsic concept of covariance function for Riemannian functional data. An estimator for the covariance function from sparsely observed Riemannian functional data is detailed in Section 3, and its theoretical properties are given in Section 4. Simulation studies are placed in Section 5, followed by an application to longitudinal diffusion tensors in Section 6.

2 Covariance vector bundle

2.1 Preliminaries

In this section we briefly review concepts from Riemannian manifolds that are essential for our development, while refer readers to the introductory text by Lee (1997) for further exposition.

Let \mathcal{M} be a d -dimensional topological manifold, which by definition is a topological space such that, for each point in \mathcal{M} there is a homeomorphism¹ between a neighborhood of the point and an open ball of \mathbb{R}^d . A smooth atlas on \mathcal{M} is a collection of pairs (U_α, ϕ_α) that are indexed by an index set J and satisfy the following axioms:

- Each U_α is an open subset of \mathcal{M} and $\bigcup_{\alpha \in J} U_\alpha = \mathcal{M}$, i.e., the domains U_α together cover \mathcal{M} .
- Each ϕ_α is a homeomorphism between U_α and the open set $\phi_\alpha(U_\alpha) = \{\phi_\alpha(x) \in \mathbb{R}^d : x \in U_\alpha\}$ of \mathbb{R}^d .
- For each pair of $\alpha, \beta \in J$, if $U_\alpha \cap U_\beta \neq \emptyset$, then the transition map $\phi_\alpha \circ \phi_\beta^{-1} : \phi_\beta(U_\alpha \cap U_\beta) \rightarrow \phi_\alpha(U_\alpha \cap U_\beta)$, illustrated in Figure 2, is smooth, i.e., infinitely differentiable; we say ϕ_α and ϕ_β are compatible.

The pair (U_α, ϕ_α) or sometimes ϕ_α itself is called a chart (or coordinate map). Two atlases are compatible if their union is again an atlas (satisfying the above axioms). An atlas is maximal if it contains any other atlas compatible with it. The space \mathcal{M} together with a smooth maximal atlas is called a smooth manifold, or simply manifold in this paper. Every point in a d -dimensional manifold is associated with a d -dimensional vector space, called the tangent space at the point. In addition, any chart (U_α, ϕ_α) gives rise to a basis for the tangent space at each point in U_α , and the basis smoothly varies with the point within U_α . Tangent spaces at different points of a manifold are conceptually distinct spaces, so that their elements, called tangent vectors, are incomparable; only tangent vectors from the same tangent space are comparable.

A Riemannian manifold is a manifold equipped with a Riemannian metric $\langle \cdot, \cdot \rangle$ which defines an inner product $\langle \cdot, \cdot \rangle_p$ on the tangent space $T_p\mathcal{M}$ at each point $p \in \mathcal{M}$, with the associated norm denoted by $\|v\|_p = \sqrt{\langle v, v \rangle_p}$ for $v \in T_p\mathcal{M}$. The metric, which smoothly varies with p , induces a distance function $d_{\mathcal{M}}$ on \mathcal{M} and turns the manifold into a metric space. A geodesic in a metric space is a curve of which every sufficiently small segment is the shortest path connecting the endpoints of the segment. For $v \in T_p\mathcal{M}$, suppose that there is a geodesic $\gamma(t)$ defined on $[0, 1]$ with $\gamma(0) = p$ such that $\gamma'(0) = v$. Here, the derivative $\gamma'(0)$ of a smooth curve, well defined via the atlas of the manifold, is a tangent vector at $\gamma(0)$ and represents the velocity of the curve γ at $t = 0$. The exponential map Exp_p at $p \in \mathcal{M}$ is then defined by $\text{Exp}_p(v) = \gamma(1)$. In turn, for each $v \in T_p\mathcal{M}$, $\gamma_v(t) := \text{Exp}_p(tv)$ defines a geodesic. The inverse of Exp_p , when it exists, is called

¹A function between two topological spaces is homeomorphic if it is continuous and bijective, and its inverse is also continuous.

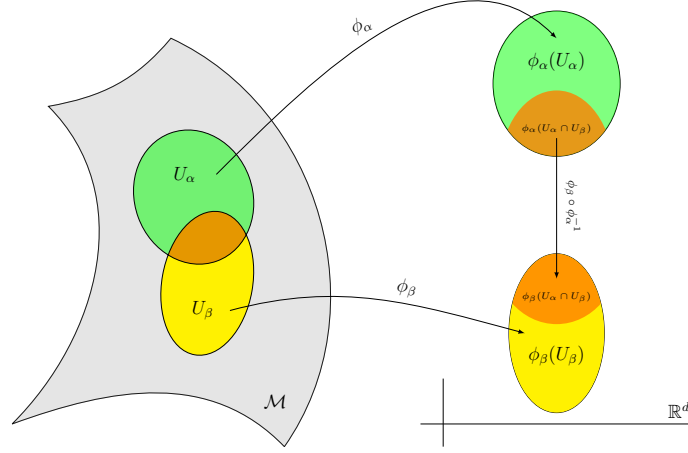


Figure 2: Illustration of the chart and transition map.

the Riemannian logarithmic map at p and denoted by Log_p ; see the left panel of Figure 3 for a graphical illustration.

In statistical analysis, it is still sometimes desirable to compare the incomparable tangent vectors from different tangent spaces. To this end, one may transport the tangent vectors into a common tangent space in which tangent vectors can be directly compared by vector subtraction. For a Riemannian manifold, there is a unique (parallel) transport associated with the Riemannian metric². In this paper, we exclusively consider parallel transport along shortest geodesics between two points y and z , denoted by \mathcal{P}_y^z , which moves tangent vectors from the tangent space $T_y\mathcal{M}$ to $T_z\mathcal{M}$ in a smooth way and meanwhile preserves the inner product; see the right panel of Figure 3 for a graphical illustration.

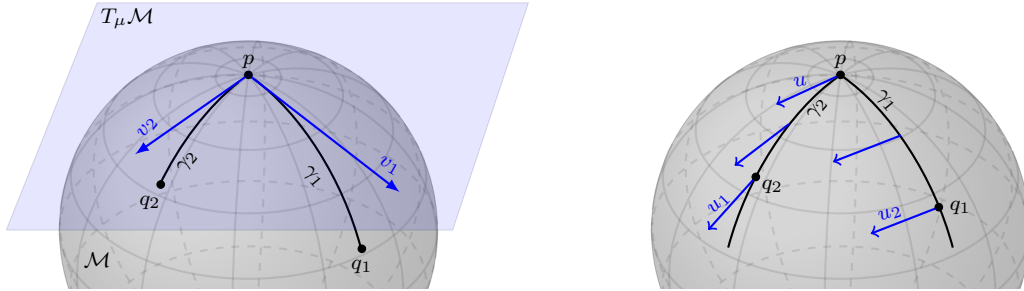


Figure 3: Left: Illustration of the tangent space, geodesic, Riemannian exponential map and logarithmic map, where $\gamma_j(0) = p$, $\gamma_j'(0) = v_j$, $\gamma_j(1) = q_j$, $q_j = \text{Exp}_p v_j$ and $v_j = \text{Log}_p q_j$, for $j = 1, 2$. Right: Illustration of parallel transport. The tangent vector u at p is parallelly transported along geodesics γ_1 and γ_2 to q_1 and q_2 , resulting in tangent vectors u_1 and u_2 , respectively.

A smooth vector bundle, denoted by $\pi : \mathcal{E} \rightarrow \mathcal{M}$ or simply \mathcal{E} , consists of a base smooth manifold \mathcal{M} , a smooth manifold \mathcal{E} called total space, and a smooth bundle projection π , such that for every $p \in \mathcal{M}$, the fiber $\pi^{-1}(p)$ is a k -dimensional real vector space, and there is an open neighborhood $U \subset \mathcal{M}$ of p and a

²The unique parallel transport is indeed determined by the Levi-Civita connection.

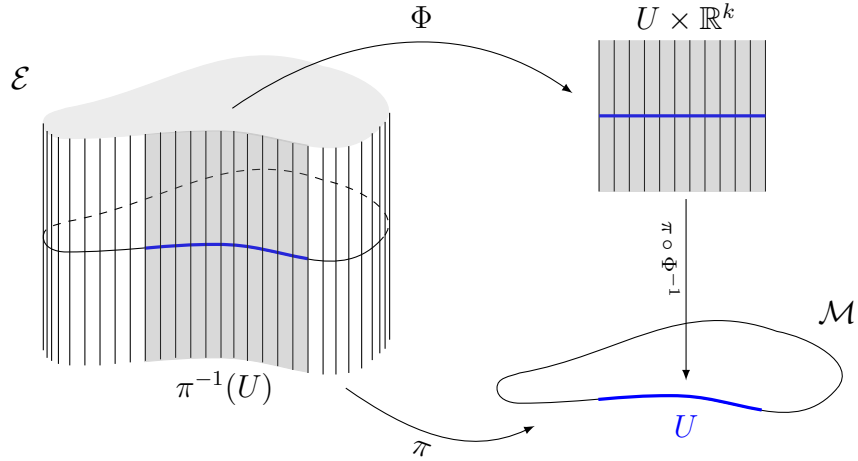


Figure 4: Illustration of the vector bundle. The closed curve in the bottom represents the base manifold \mathcal{M} and the figure on the left represents the total space \mathcal{E} , where each vertical line represents a fiber. The thickened segment $U \subset \mathcal{M}$ represents an open subset of the manifold \mathcal{M} , while Φ is a local trivialization defined on $\pi^{-1}(U)$ that is highlighted in gray in the total space.

diffeomorphism³ $\Phi : \pi^{-1}(U) \rightarrow U \times \mathbb{R}^k$ satisfying the property that for all $z \in U$, $(\pi \circ \Phi^{-1})(z, v) = z$ for all $v \in \mathbb{R}^k$ and the map $v \mapsto \Phi^{-1}(z, v)$ is a linear isomorphism between \mathbb{R}^k and $\pi^{-1}(z)$. The map Φ is called a local trivialization. As graphically illustrated in Figure 4, a vector bundle locally resembles the product space $U \times \mathbb{R}^k$ for some integer k . A prominent example of vector bundle is the space composed by the union of all tangent spaces of a manifold, which is called the tangent bundle of the manifold, where the tangent space at each point is a fiber. To identify different fibers, one can introduce a parallel transport \mathcal{P} on a vector bundle along a geodesic curve γ on the base manifold. Such parallel transport must satisfy the following axioms: 1) \mathcal{P}_p^p is the identity map on $\pi^{-1}(p)$ for all $p \in \mathcal{M}$, 2) $\mathcal{P}_{\gamma(u)}^{\gamma(t)} \circ \mathcal{P}_{\gamma(s)}^{\gamma(u)} = \mathcal{P}_{\gamma(s)}^{\gamma(t)}$, and 3) the dependence of \mathcal{P} on γ , s and t are smooth. The parallel transport \mathcal{P} introduced previously for a Riemannian manifold is indeed a parallel transport on the tangent bundle. In Section 2.4 we will construct a new type of vector bundle and a parallel transport on it. If for each fiber in a smooth vector bundle there is an inner product and the inner product smoothly varies from fiber to fiber, then the inner products are collectively referred to as a smooth bundle metric. The aforementioned Riemannian metric is indeed a smooth bundle metric on the tangent bundle.

2.2 Riemannian functional data

Functional data in which each function takes values in a Riemannian manifold are termed Riemannian functional data and modeled by the Riemannian random process (Lin and Yao, 2019). Specifically, let \mathcal{M} be a d -dimensional smooth Riemannian manifold and X a \mathcal{M} -valued random process indexed by a compact domain $\mathcal{T} \in \mathbb{R}$, i.e., $X : \mathcal{T} \times \Omega \rightarrow \mathcal{M}$, where Ω is the sample space of the underlying probability space. In reality, measurements of X are often corrupted by noise. To accommodate this common practice, we assume that the actual observable process is Y which is indexed by the same domain \mathcal{T} .

The process X is said to be of second order, if for each $t \in \mathcal{T}$, $F(p, t) = \mathbf{E}d_{\mathcal{M}}^2(X(t), p) < \infty$ for some $p \in \mathcal{M}$ and hence for all $p \in \mathcal{M}$ due to the triangle inequality. The minimizer of $F(p, t)$, if it exists, is called the

³A diffeomorphism is a smooth bijective function between two smooth manifolds.

Fréchet mean of $X(t)$ and denoted by $\mu(t)$, i.e.,

$$\mu(t) := \arg \min_{p \in \mathcal{M}} F(p, t). \quad (1)$$

The concept of the Fréchet mean generalizes the mean from the Euclidean space to the Riemannian manifold and plays an important role in analysis of data residing in a Riemannian manifold. Under fairly general conditions, the Fréchet mean exists and is unique (Bhattacharya and Patrangenaru, 2003; Sturm, 2003; Afsari, 2011), for instance, when the manifold is of nonpositive sectional curvature (p.146, Lee, 1997) or data are located in a small subspace of the manifold. Formally, we make the following assumption.

Assumption 2.1. *The Fréchet mean functions of X and Y exist and are unique.*

As the manifold \mathcal{M} is not a vector space, it is challenging to directly study the processes X and Y . A common strategy to circumvent this difficulty is to transform them into tangent spaces, in which the vector structure can facilitate the analysis, via Riemannian logarithmic maps. This requires an additional assumption to ensure the well-posedness of the Riemannian logarithmic maps. For simplicity, we assume the following sufficient condition, which can be relaxed by a delicate formulation via cut locus⁴.

Assumption 2.2. *There exists a geodesically convex⁵ subset $\mathcal{Q} \subset \mathcal{M}$ such that $X(t), Y(t) \in \mathcal{Q}$ for all $t \in \mathcal{T}$.*

If the manifold is simply connected and of nonpositive sectional curvature, \mathcal{Q} can be taken to be \mathcal{M} and thus the above assumption becomes superfluous. Examples of manifolds of this kind include hyperbolic manifolds, tori and the space of symmetric positive-definite matrices endowed with the affine-invariant metric (Moakher, 2005), Log-Euclidean metric (Arsigny et al., 2007) or Log-Cholesky metric (Lin, 2019). An example \mathcal{Q} for Riemannian manifolds whose sectional curvature is not nonnegative is the positive orthant $\mathcal{Q} = \{(x_0, \dots, x_k) \in \mathbb{S}^k : x_j \geq 0 \text{ for all } j = 0, \dots, k\}$ in the hypersphere $\mathbb{S}^k = \{(x_0, \dots, x_k) \in \mathbb{R}^{k+1} : x_0^2 + \dots + x_k^2 = 1\}$, which has applications in compositional data analysis (Dai and Müller, 2018), where k is a positive integer. Under Assumptions 2.1 and 2.2, the Riemannian logarithmic maps $\text{Log}_{\mu(t)}\{X(t)\}$ and $\text{Log}_{\mu(t)}\{Y(t)\}$ are well defined. In addition, we can further model the observed process by $Y(t) = \text{Exp}_{\mu(t)}(\text{Log}_{\mu(t)}\{X(t)\} + \varepsilon(t))$, where $\varepsilon(t) \in T_{\mu(t)}\mathcal{M}$ represents the random noise in the tangent space, is independent of X , and satisfies $\mathbf{E}\varepsilon(t) = 0$ and $\text{Exp}_{\mu(t)}\varepsilon(t) \in \mathcal{Q}$. We shall see later that the mean functions of X and Y are the same.

Now we are ready to model sparsely observed Riemannian functional data. First, the sample functions X_1, \dots, X_n are considered as i.i.d. realizations of X . However, accessible are their noisy copies Y_1, \dots, Y_n , rather than X_1, \dots, X_n . To further accommodate the practice that functions are often only recorded at discrete points, we assume each Y_i is only observed at m_i time points $T_{i,1}, \dots, T_{i,m_i} \in \mathcal{T}$ with $T_{ij} \stackrel{i.i.d.}{\sim} T$, where T is a random variable in \mathcal{T} . Specifically, the observations are $\{(T_{ij}, Y_{ij}) \in \mathcal{T} \times \mathcal{M} : 1 \leq i \leq n, 1 \leq j \leq m_i\}$ with $Y_{ij} = \text{Exp}_{\mu(T_{ij})}(\text{Log}_{\mu(T_{ij})}\{X_i(T_{ij})\} + \varepsilon_{ij})$, where the centered random elements $\varepsilon_{ij} \in T_{\mu(T_{ij})}\mathcal{M}$ are independent of each other and also independent of $\{X_i : 1 \leq i \leq n\}$ and $\{T_{kl} : 1 \leq k \leq n, 1 \leq l \leq m_i\} \setminus \{T_{ij}\}$. In addition, $\{T_{kl} : 1 \leq k \leq n, 1 \leq l \leq m_i\}$ is independent of $\{X_i : 1 \leq i \leq n\}$. The assumed independence and identical distributions in the above can be relaxed at the cost of much heavier technicalities. Such relaxation does not lead to additional insight and thus is not pursued in this article.

⁴Roughly speaking, the cut locus of a point p in a manifold is the collection of points q of the manifold such that $\text{Log}_p q$ is not uniquely defined.

⁵A subset in a Riemannian manifold is geodesically convex if for any two points in the subset there is a unique shortest geodesic that is contained in the subset and connects the points.

2.3 Covariance function of Riemannian functional data

In addition to the Fréchet mean function, the covariance structure of Riemannian functional data is essential for downstream analysis, for instance, functional principal component analysis. In Lin and Yao (2019) the covariance structure is modeled by the covariance operator of $\text{Log}_{\mu(\cdot)}X(\cdot)$ from the random element perspective (Chapter 7, Hsing and Eubank, 2015) and also by the covariance function of $\text{Log}_{\mu(\cdot)}X(\cdot)$ with respect to a frame⁶. The covariance operator is not computationally friendly to sparse data while the frame-dependent covariance function is not compatible with most smoothing methods; see Remark 3.1 for details.

To develop a frame-independent intrinsic concept of the covariance function from the perspective of stochastic processes, we first revisit the covariance between two centered random vectors U and V . When they are in a common Euclidean space, it is classically defined as the matrix $\mathbf{E}(UV^\top)$. When U and V are in different general inner product spaces \mathbb{U} and \mathbb{V} , a matrix representation of the covariance is definable if one picks an orthonormal basis for each of \mathbb{U} and \mathbb{V} . To eliminate the dependence on the orthonormal bases, we take an operator perspective to treat the covariance C of U and V as a linear operator between \mathbb{U} and \mathbb{V} characterized by

$$\langle Cu, v \rangle_{\mathbb{V}} := \mathbf{E}(\langle U, u \rangle_{\mathbb{U}} \langle V, v \rangle_{\mathbb{V}}), \quad \forall u \in \mathbb{U}, v \in \mathbb{V},$$

where $\langle \cdot, \cdot \rangle_{\mathbb{U}}$ and $\langle \cdot, \cdot \rangle_{\mathbb{V}}$ denote the inner products of \mathbb{U} and \mathbb{V} , respectively. To simplify the notation, we write $C = \mathbf{E}(U \otimes V)$.

Observe that $\text{Log}_{\mu(\cdot)}X(\cdot)$ ($\text{Log}_{\mu}X$ for short) is a random vector field along the curve μ with $\mathbf{E}(\text{Log}_{\mu}X) = 0$ (Theorem 2.1, Bhattacharya and Patrangenaru, 2003). Given that $\text{Log}_{\mu(s)}X(s) \in T_{\mu(s)}\mathcal{M}$ and $\text{Log}_{\mu(t)}X(t) \in T_{\mu(t)}\mathcal{M}$, and both $T_{\mu(s)}\mathcal{M}$ and $T_{\mu(t)}\mathcal{M}$ are Hilbert spaces, we define the covariance function for X at time (s, t) by

$$\mathcal{C}(s, t) := \mathbf{E}\{\text{Log}_{\mu(s)}X(s) \otimes \text{Log}_{\mu(t)}X(t)\}. \quad (2)$$

This covariance function is clearly *independent* of any frame or coordinate system. This feature fundamentally and distinctly separates (2) from the frame-dependent covariance function (5) defined in Lin and Yao (2019) for the coordinate of $\text{Log}_{\mu}X$ with respect to a frame along the mean function. Moreover, (2) can be viewed as the intrinsic covariance function of the covariance operator \mathbf{C} proposed in Lin and Yao (2019). Specifically, under some measurability or continuity assumption on X and the condition that $\mathbf{E} \int_{\mathcal{T}} \|\text{Log}_{\mu(t)}X(t)\|_{\mu(t)}^2 < \infty$, the process $\text{Log}_{\mu}X$ can be regarded as a random element in the Hilbert space $\mathcal{T}(\mu) := \{Z : Z(\cdot) \in T_{\mu(\cdot)}\mathcal{M}, \int_{\mathcal{T}} \langle Z(t), Z(t) \rangle_{\mu(t)} dt < \infty\}$ endowed with the inner product $\langle\langle Z_1, Z_2 \rangle\rangle_{\mu} := \int_{\mathcal{T}} \langle Z_1(t), Z_2(t) \rangle_{\mu(t)} dt$ for $Z_1, Z_2 \in \mathcal{T}(\mu)$. The covariance operator $\mathbf{C} : \mathcal{T}(\mu) \rightarrow \mathcal{T}(\mu)$ for X can be defined by

$$\langle\langle \mathbf{C}u, v \rangle\rangle_{\mu} := \mathbf{E}(\langle\langle \text{Log}_{\mu}X, u \rangle\rangle_{\mu} \langle\langle \text{Log}_{\mu}X, v \rangle\rangle_{\mu}) \quad \text{for } u, v \in \mathcal{T}(\mu). \quad (3)$$

The following theorem, which generalizes Theorem 7.4.3 of Hsing and Eubank (2015) to Riemannian random processes, shows that the proposed covariance function induces the covariance operator \mathbf{C} .

Theorem 2.1. *Let $\mathcal{C}(\cdot, \cdot)$ and \mathbf{C} be defined in (2) and (3), respectively. Suppose that X is mean-square continuous, i.e., $\lim_{k \rightarrow \infty} \mathbf{E}d^2(X(t_k), X(t)) = 0$ for any $t \in \mathcal{T}$ and any sequence $\{t_k\}$ in \mathcal{T} converging to t . Also assume that X is jointly measurable, i.e., $X : \mathcal{T} \times \Omega \rightarrow \mathcal{M}$ is measurable with respect to the product σ -field on $\mathcal{T} \times \Omega$, where Ω is the sample space of the underlying probability space. Then under Assumptions*

⁶Recall that a frame specifies a basis for each tangent space.

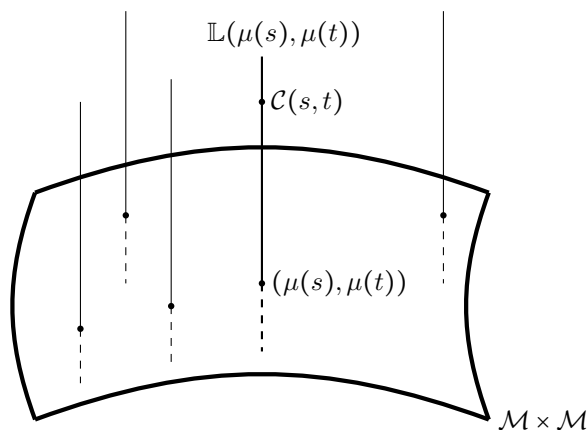


Figure 5: Illustration of the vector bundle \mathbb{L} . The thick bending parallelogram presents the product manifold $\mathcal{M} \times \mathcal{M}$ and the vertical lines represent fibers. The value of $\mathcal{C}(s, t)$ is located within the fiber $\mathbb{L}(\mu(s), \mu(s))$ at the point $(\mu(s), \mu(t)) \in \mathcal{M} \times \mathcal{M}$.

2.1 and 2.2, for all $t \in \mathcal{T}$ and $u \in \mathcal{F}(\mu)$, we have

$$(\mathbf{C}u)(t) = \int_{\mathcal{T}} \mathcal{C}(s, t)u(s)ds.$$

In light of this result, in the sequel we use the same notation \mathcal{C} to denote both the covariance operator and the covariance function in (2). The proposed covariance function enables us to estimate the covariance operator \mathbf{C} through estimating $\mathcal{C}(s, t)$ for each $(s, t) \in \mathcal{T} \times \mathcal{T}$ in a frame-independent fashion. The frame-independent feature is of particular importance to deriving a frame-invariant estimate in the more practical scenario that only discrete and noisy observations are available so that smoothing is desirable; see Section 3 for details.

2.4 The vector bundle of covariance and parallel transport

To estimate the covariance function in (2), it seems rather intuitive to perform smoothing over the raw covariance function $\hat{\mathcal{C}}_{i,jk} := \text{Log}_{\hat{\mu}(T_{ij})}Y_{ij} \otimes \text{Log}_{\hat{\mu}(T_{ik})}Y_{ik}$, where $\hat{\mu}$ is an estimate of μ to be detailed in Section 3. The first challenge encountered is that these raw observations $\hat{\mathcal{C}}_{i,jk}$ do not reside in a common vector space. This also gives rise to the second challenge in defining the critical concept of *smoothness* of the function \mathcal{C} and its estimate. To circumvent these difficulties, we consider the spaces $\mathbb{L}(p, q)$ consisting of all linear maps from $T_p\mathcal{M}$ to $T_q\mathcal{M}$, and their disjoint union $\mathbb{L} = \bigcup_{(p,q) \in \mathcal{M}^2} \mathbb{L}(p, q)$. Then $\hat{\mathcal{C}}_{i,jk}$ are encompassed by the space \mathbb{L} , and in addition, the covariance function \mathcal{C} is now viewed as a \mathbb{L} -valued function. Although the space \mathbb{L} is not a vector space so that the smoothness is not definable in the classic sense, we observe that \mathbb{L} comes with a canonical smooth structure induced by the manifold \mathcal{M} , and continuity, differentiability and smoothness relevant to statistics can be defined with reference to this smooth structure, as follows.

We first observe that \mathbb{L} is a vector bundle on $\mathcal{M} \times \mathcal{M}$, with $\pi : \mathbb{L} \rightarrow \mathcal{M} \times \mathcal{M}$ defined by $\pi(\mathbb{L}(p, q)) = (p, q)$ being the bundle projection and $\mathbb{L}(p, q)$ being the fiber attached to the point $(p, q) \in \mathcal{M} \times \mathcal{M}$; see Figure 5 for a graphical illustration. To define the smoothness structure on \mathbb{L} induced by the manifold \mathcal{M} , let $\{(U_\alpha, \phi_\alpha) : \alpha \in J\}$ for an index set J be an atlas of \mathcal{M} . Recall that each chart (U_α, ϕ_α) gives rise to a smoothly varying basis of $T_p\mathcal{M}$ for each $p \in U_\alpha$. Such basis is denoted by $B_{\alpha,1}(p), \dots, B_{\alpha,d}(p)$. For $(p, q) \in U_\alpha \times U_\beta$, the tensor products $B_{\alpha,j}(p) \otimes B_{\beta,k}(q)$, $j, k = 1, \dots, d$, form a basis for the space $\mathbb{L}(p, q)$. Each element $v \in \mathbb{L}(p, q)$ is then identified with its coefficients v_{jk} with respect to this basis, i.e., $v = \sum_{j,k=1}^d v_{jk} B_{\alpha,j}(p) \otimes B_{\beta,k}(q)$. For each

$U_\alpha \times U_\beta$, we define the map $\varphi_{\alpha,\beta}(p, q, \sum_{j,k=1}^d v_{jk} B_{\alpha,j}(p) \otimes B_{\beta,k}(q)) = (\phi_\alpha(p), \phi_\beta(q), v_{11}, v_{12}, \dots, v_{dd}) \in \mathbb{R}^{2d+d^2}$, for $(p, q) \in U_\alpha \times U_\beta$. The collection $\{(\pi^{-1}(U_\alpha \times U_\beta), \varphi_{\alpha,\beta}) : (\alpha, \beta) \in \mathcal{J}^2\}$ indeed is a smooth atlas that turns \mathbb{L} into a smooth manifold. Moreover, \mathbb{L} is a *smooth* vector bundle with the projection map π and the local trivializations $\Phi_{\alpha,\beta} : \pi^{-1}(U_\alpha \times U_\beta) \rightarrow U_\alpha \times U_\beta \times \mathbb{R}^{d^2}$ defined as $\Phi_{\alpha,\beta}(p, q, \sum_{j,k=1}^d v_{jk} B_{\alpha,j}(p) \otimes B_{\beta,k}(q)) = (p, q, v_{11}, v_{12}, \dots, v_{dd})$.

Theorem 2.2. *The collection $\{(\pi^{-1}(U_\alpha \times U_\beta), \varphi_{\alpha,\beta}) : (\alpha, \beta) \in \mathcal{J}^2\}$ is a smooth atlas on \mathbb{L} . With this atlas, \mathbb{L} is a smooth vector bundle with the smooth projection map π and smooth local trivializations $\Phi_{\alpha,\beta}$. In addition, any compatible atlas of the manifold \mathcal{M} gives rise to the same smooth vector bundle \mathbb{L} .*

With the above smooth structure, the covariance function \mathcal{C} in (2), viewed as an \mathbb{L} -valued function, is said to be κ -times continuously differentiable in (s, t) , if $(\mu(s), \mu(t)) \in U_\alpha \times U_\beta$ implies that $\varphi_{\alpha,\beta}(\mu(s), \mu(t), \mathcal{C}(s, t))$ is κ -times continuously differentiable in (s, t) , where we recall that $\{(\pi^{-1}(U_\alpha \times U_\beta), \varphi_{\alpha,\beta}) : (\alpha, \beta) \in \mathcal{J}^2\}$ is a smooth atlas on \mathbb{L} . From this perspective, the constructed vector bundle \mathbb{L} provides a framework to rigorously define the regularity of \mathcal{C} . In this framework, estimating the covariance function \mathcal{C} is amount to smoothing the discrete raw observations $\hat{\mathcal{C}}_{i,jk}$ in the vector bundle \mathbb{L} .

Although the vector bundle \mathbb{L} provides a qualitative framework for defining differentiability or other smoothness regularity, it does not provide a quantitative characterization. Roughly speaking, the smooth vector bundle \mathbb{L} allows one to check whether \mathcal{C} is differentiable or smooth, but not to measure how rapidly \mathcal{C} changes relative to (s, t) . In other words, derivatives, that quantify the rate of change of the function \mathcal{C} at a given pair (s, t) and that are consistent across all compatible atlases for \mathbb{L} , require an additional structure, as follows. We first introduce the parallel transport on the covariance vector bundle \mathbb{L} to identify different fibers and to compare the elements from the fibers. Suppose that $(p_1, q_1), (p_2, q_2) \in \mathcal{M} \times \mathcal{M}$ and $\gamma(t) = (\gamma_p(t), \gamma_q(t))$ is a shortest geodesic connecting (p_1, q_1) to (p_2, q_2) . The parallel transport $\mathcal{P}_{(p_1, q_1)}^{(p_2, q_2)}$ from a fiber $\mathbb{L}(p_1, q_1)$ to another fiber $\mathbb{L}(p_2, q_2)$ along the curve $\gamma(t)$ is naturally constructed from the parallel transport operators $\mathcal{P}_{p_2}^{p_1}$ and $\mathcal{P}_{q_1}^{q_2}$ on \mathcal{M} by

$$(\mathcal{P}_{(p_1, q_1)}^{(p_2, q_2)} \mathcal{C})(u) := \mathcal{P}_{q_1}^{q_2}(\mathcal{C}(\mathcal{P}_{p_2}^{p_1} u)), \quad (4)$$

where $C \in \mathbb{L}(p_1, q_1)$ and $u \in T_{p_2} \mathcal{M}$. To distinguish between the parallel transport on the manifold and the one on the vector bundle \mathbb{L} , notationally we use the calligraphic symbol \mathcal{P} for the manifold while the script symbol \mathcal{P} for the bundle. The parallel transport \mathcal{P} further determines a covariant derivative on the bundle. For a definition of covariant derivatives, see Chapter 4 (specifically, Page 50) of Lee (1997).

Theorem 2.3. *For a tangent vector V of $\mathcal{M} \times \mathcal{M}$ at (p, q) , the map ∇_V defined by*

$$\nabla_V W := \lim_{h \rightarrow 0} \frac{\mathcal{P}_{\gamma(h)}^{\gamma(0)} W(\gamma(h)) - W(\gamma(0))}{h} := \frac{d}{dt} \mathcal{P}_{\gamma(t)}^{\gamma(0)} W(\gamma(t)) \Big|_{t=0} \quad \text{for all differentiable section } W \quad (5)$$

is a covariant derivative in the direction of V , where γ is a geodesic in $\mathcal{M} \times \mathcal{M}$ with initial point $\gamma(0) = (p, q)$ and initial velocity $\gamma'(0) = V$, and a section is any function $W : \mathcal{M} \times \mathcal{M} \rightarrow \mathbb{L}$ satisfying $W(p, q) \in \mathbb{L}(p, q)$ for all $(p, q) \in \mathcal{M} \times \mathcal{M}$.

The covariant derivative of a section W can be viewed as the first derivative of the section. It quantifies the rate and direction of change of W at each point in $\mathcal{M} \times \mathcal{M}$. This applies to the covariance function \mathcal{C} since it can be viewed as a section along the surface $\mu \times \mu : \mathcal{T} \times \mathcal{T} \rightarrow \mathcal{M} \times \mathcal{M}$. For example, the ‘‘partial derivative’’ $\frac{\partial}{\partial s} \mathcal{C}(s, t) \Big|_{s=s_0}$ of $\mathcal{C}(s, t)$ with respect to s is defined as the covariant derivative of $\mathcal{C}(s, t)$ in the direction $V = \eta'(s_0)$ with $\eta(s) = (\mu(s), \mu(t))$ being a curve on $\mathcal{M} \times \mathcal{M}$. Furthermore, since the derivative

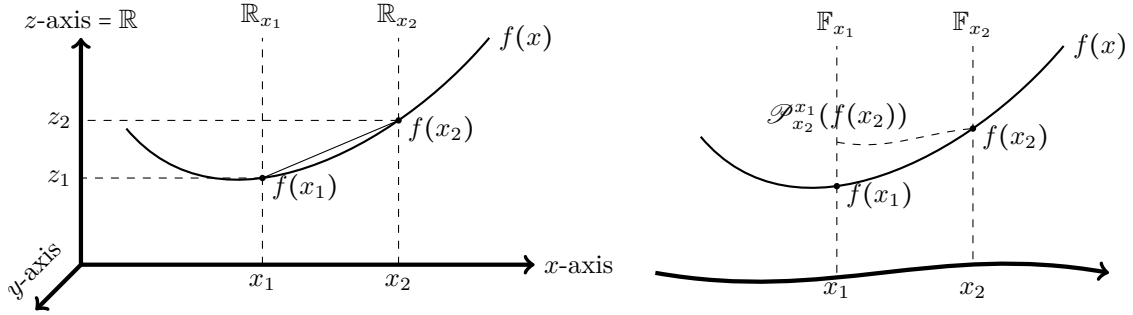


Figure 6: Illustration of classic differentiation (left) and general covariant derivative (right).

$\frac{\partial}{\partial s}\mathcal{C}(s, t)$ is again a section of the vector bundle, one can define the partial derivatives of $\frac{\partial}{\partial s}\mathcal{C}(s, t)$, which can be regarded as the second derivatives of \mathcal{C} . Higher-order derivatives can be defined in a recursive way.

To further illustrate the parallel transport and the induced covariant derivative on the vector bundle $\pi : \mathbb{L} \rightarrow \mathcal{M} \times \mathcal{M}$, consider a simple example in which $\mathcal{M} = \mathbb{R}$ and the bundle \mathbb{L} is then parameterized by $(x, y, z) \in \mathbb{R}^2 \times \mathbb{R}$. Let $g : \mathcal{M} \times \mathcal{M} \rightarrow \mathbb{L}$ be a smooth section. For visualization, we fix $y = 0$ and write $f(x) = g(x, 0)$. For the smooth function $f(x)$ shown in Figure 6, the classic definition of the derivative of $f(x)$ at x_1 is

$$\left. \frac{\partial}{\partial x} f(x) \right|_{x=x_1} := \lim_{x_2 \rightarrow x_1} \frac{f(x_2) - f(x_1)}{x_2 - x_1}.$$

From the perspective of the vector bundle, each point x in the x -axis is attached with a fiber \mathbb{R}_x which is simply a copy of the z -axis $= \mathbb{R}$. Since $f(x_1) \in \mathbb{R}_{x_1}$ while $f(x_2) \in \mathbb{R}_{x_2}$, the operation $f(x_2) - f(x_1)$ would not be well defined if we did not identify \mathbb{R}_{x_1} with \mathbb{R}_{x_2} . The identification between \mathbb{R}_{x_1} and \mathbb{R}_{x_2} is canonical, and nothing else but parallelly transporting \mathbb{R}_{x_2} to \mathbb{R}_{x_1} . This inspiring observation applies to general manifolds and covariant derivatives. Specifically, the covariant derivative is defined by parallel transporting $f(x_2)$ from the fiber \mathbb{F}_{x_2} into the fiber \mathbb{F}_{x_1} and then performing differentiation therein, i.e.,

$$\left. \frac{\partial}{\partial x} f(x) \right|_{x=x_1} := \lim_{x_2 \rightarrow x_1} \frac{\mathcal{P}_{x_2}^{x_1}(f(x_2)) - f(x_1)}{x_2 - x_1} \in \mathbb{F}_{x_1}.$$

Finally, when smoothing the raw covariance function $\hat{\mathcal{C}}_{i,jk}$, one needs to quantify the discrepancy between the data and the fitted. Such discrepancy is often measured by a distance function or inner product on the data space. Fortunately, the vector bundle \mathbb{L} comes with a natural bundle metric. Specifically, for any $(p, q) \in \mathcal{M} \times \mathcal{M}$, the inner product $G_{(p,q)} : \mathbb{L}(p, q) \times \mathbb{L}(p, q) \rightarrow \mathbb{R}$ is defined as the Hilbert–Schmidt inner product, i.e.,

$$G_{(p,q)}(L_1, L_2) = \sum_{k=1}^d \langle L_1 e_k, L_2 e_k \rangle_q \quad \text{for } L_1, L_2 \in \mathbb{L}(p, q), \quad (6)$$

where e_1, \dots, e_d denotes an orthonormal basis of $T_p\mathcal{M}$. One can show that the definition (6) does not depend on the choice of the orthonormal basis. In fact, G is a smooth bundle metric and the parallel transport (4) defines an isometry between any two fibers, as asserted by the following result.

Theorem 2.4. *The metric defined in (6) is a vector bundle metric that smoothly varies with $(p, q) \in \mathcal{M} \times \mathcal{M}$ and is preserved by the parallel transport in (4).*

The inner product (6) is defined for linear operators that map a Hilbert space, such as $T_p\mathcal{M}$, to another potentially different Hilbert space, such as $T_q\mathcal{M}$. The inner product of this type, although mathematically well established (e.g., Definition 2.3.3 and Proposition B.0.7 by Prévôt and Röckner, 2007), is less seen in

statistics; the common one is defined for linear operators that map a Hilbert space into the same Hilbert space. The metric G also induces a norm, denoted by $\|\cdot\|_{G(p,q)}$ or simply $\|\cdot\|_G$, on each fiber $\mathbb{L}(p,q)$. This norm in turn defines a distance on each fiber $\mathbb{L}(p,q)$ by $\|A-B\|_{G(p,q)}$ for $A, B \in \mathbb{L}(p,q)$, which is an integrated part of the loss function in (7) for estimating the covariance function.

The smooth vector bundle \mathbb{L} together with the covariant derivative (5) and the bundle metric (6), termed *covariance vector bundle* in this paper, paves the way for estimation of the covariance function (2) from sparsely observed Riemannian functional data. The smooth structure and the covariant derivative together provide an intrinsic mechanism to quantify the regularity of \mathcal{C} . For example, it makes meaningful the statement that the second derivatives of $\mathcal{C}(s,t)$ are continuous. In the Euclidean case, statements of this kind are often adopted as assumptions that are fundamental to theoretical analysis of estimators derived from a smoothing method. The developed vector bundle and covariant derivative now enable us to extend such assumptions to the manifold setting, as demonstrated in Section 4.2 where we analyze the theoretical properties of our estimators proposed in Section 3 for the covariance function \mathcal{C} . The parallel transport (4) and the bundle metric (6) allow an intrinsic measure of the discrepancy of objects in the covariance vector bundle. Such measure is critical for finding an estimator for \mathcal{C} and quantifying the quality of the estimator, as illustrated in the following sections.

3 Estimation

The first step is to estimate the mean function, for which we adopt the local linear regression method proposed by Petersen and Müller (2019) and also employed by Dai et al. (2020), as follows. Define the local weight function

$$\hat{w}(T_{ij}, t, h_\mu) = \frac{1}{\hat{\sigma}_0^2(t)} K_{h_\mu}(T_{ij} - t) \{\hat{u}_2(t) - \hat{u}_1(t)(T_{ij} - t)\},$$

where $\hat{u}_k(t) = \sum_i \lambda_i \sum_j K_{h_\mu}(T_{ij} - t)(T_{ij} - t)^k$, $\hat{\sigma}_0^2(t) = \hat{\mu}_0(t)\hat{\mu}_2(t) - \hat{\mu}_1^2(t)$ and $K_{h_\mu}(\cdot) = K(\cdot/h_\mu)/h_\mu$ for a kernel function K with bandwidth $h_\mu > 0$. The estimate $\hat{\mu}$ is defined as the minimizer of the weighted function

$$\hat{Q}_n(y, t) = \sum_{1 \leq i \leq n} \lambda_i \sum_{1 \leq j \leq m_i} \hat{w}(T_{ij}, t, h) d_{\mathcal{M}}^2(Y_{ij}, y),$$

i.e.,

$$\hat{\mu}(t) = \arg \min_{y \in \mathcal{M}} \hat{Q}_n(y, t),$$

where the weights $\{\lambda_i\}_{1 \leq i \leq n}$ are subject-specific and satisfy $\sum_{i=1}^n \lambda_i m_i = 1$. For the Euclidean case $\mathcal{M} = \mathbb{R}$, the objective function $\hat{Q}_n(y, t)$ coincides with the sum of squared error loss used in Zhang and Wang (2016). Two popular choices for λ_i are $\lambda_i = \frac{1}{\sum_{i=1}^n m_i}$ (Yao et al., 2005) that assigns equal weight to each observation, and $\lambda_i = \frac{1}{nm_i}$ (Li and Hsing, 2010) that assigns equal weight to each subject. Further choices are discussed in Zhang and Wang (2018).

Given the parallel transport introduced in Section 2.4, we are allowed to move raw observations $\hat{\mathcal{C}}_{i,jk}$ from different fibers into the same fiber and employ the classic local linear smoothing on the transported observations. Recall that the raw covariance is defined by

$$\hat{\mathcal{C}}_{i,jk} := \text{Log}_{\hat{\mu}(T_{ij})} Y_{ij} \otimes \text{Log}_{\hat{\mu}(T_{ik})} Y_{ik} \in \mathbb{L}(\hat{\mu}(T_{ij}), \hat{\mu}(T_{ik})).$$

For the above to be well defined, similar to Assumption 2.1, we assume the existence and uniqueness of the empirical mean function $\hat{\mu}$. Such condition is not needed for manifolds of nonpositive sectional curvature,

or may be replaced by a convexity condition on the distance function when Assumption 2.2 holds.

Assumption 3.1. *The estimated mean function $\hat{\mu}(t)$ exists and is unique for each $t \in \mathcal{T}$.*

To estimate $\mathcal{C}(s, t)$, the nearby raw observations $\hat{\mathcal{C}}_{i,jk}$ are parallelly transported into the fiber $\mathbb{L}(\hat{\mu}(s), \hat{\mu}(t))$, and the estimate $\hat{\mathcal{C}}(s, t)$ is set by $\hat{\mathcal{C}}(s, t) = \hat{\beta}_0$ with

$$(\hat{\beta}_0, \hat{\beta}_1, \hat{\beta}_2) = \arg \min_{\beta_0, \beta_1, \beta_2 \in \mathbb{L}(\hat{\mu}(s), \hat{\mu}(t))} \sum_i \nu_i \sum_{j \neq k} \left\| \mathcal{P}_{(\hat{\mu}(T_{ij}), \hat{\mu}(T_{ik}))}^{(\hat{\mu}(s), \hat{\mu}(t))} \hat{\mathcal{C}}_{i,jk} - \beta_0 - \beta_1(T_{ij} - s) - \beta_2(T_{ik} - t) \right\|_{G(\hat{\mu}(s), \hat{\mu}(t))}^2 K_{h_c}(s - T_{ij}) K_{h_c}(t - T_{ik}), \quad (7)$$

where $h_c > 0$ is a bandwidth, $\mathcal{P}_{(\hat{\mu}(T_{ij}), \hat{\mu}(T_{ik}))}^{(\hat{\mu}(s), \hat{\mu}(t))}$ is the parallel transport along minimizing geodesics defined in (4), and the weights $\{\nu_i\}_{1 \leq i \leq n}$ are subject-specific and satisfy $\sum_{i=1}^n \nu_i m_i (m_i - 1) = 1$. Similar to the estimation of the mean function, two popular choices for the weights are $\nu_i = \frac{1}{\sum_{i=1}^n m_i (m_i - 1)}$ (Yao et al., 2005) that assign equal weight to each observation, and $\nu_i = \frac{1}{nm_i(m_i - 1)}$ (Li and Hsing, 2010) that assign equal weight to each subject. Further options are studied in Zhang and Wang (2018).

The objective function in (7) involves only intrinsic concepts and thus is fundamentally different from the objective function in (5) of Dai et al. (2020) in which the raw observations $\hat{\mathcal{C}}_{i,jk}$ are computed in an ambient space. In addition, the quantities $\hat{\mathcal{C}}_{i,jk}$ in (7) are frame-independent and thus the resulting estimator is invariant to the frame⁷. This frame-independent feature makes our estimator distinct from the hypothetical estimator discussed in the following Remark 3.1 in which a frame is essential and the produced estimator is not invariant to the frame.

Remark 3.1. *An “obvious” estimator for \mathcal{C} might be obtained by utilizing a frame along $\hat{\mu}(\cdot)$ and the coefficient process of Lin and Yao (2019). Specifically, fix a frame along $\hat{\mu}$ which determines an orthonormal basis of $T_{\hat{\mu}(t)}\mathcal{M}$ for each $t \in \mathcal{T}$. Then $\text{Log}_{\hat{\mu}(T_{ij})} Y_{ij}$ can be represented by its coefficient vector \hat{c}_{ij} with respect to the frame, and $\hat{\mathcal{C}}_{i,jk}$ is also represented by the observed coefficient matrix $\hat{c}_{ij} \hat{c}_{ik}^\top$. Local linear smoothing or other smoothing methods can be applied on these matrices to yield an estimated coefficient matrix at any pair (s, t) of time points, and the corresponding estimate $\hat{\mathcal{C}}(s, t)$ is recovered from the estimated coefficient matrix and the frame. However, this estimate is not invariant to the frame, i.e., different frames give rise to different estimates $\hat{\mathcal{C}}(s, t)$. The reason is that, smoothing methods optimize certain objective function of the observations which are the frame-dependent coefficient matrices $\hat{c}_{ij} \hat{c}_{ik}^\top$ in this context, while most objective functions, like sum of squared errors, are not invariant to the frame. Note that in (7) this issue is avoided by using a frame-free objective function.*

Remark 3.2. *One might attempt to endow \mathbb{L} with a distance ρ so that the estimation is turned into a regression problem with a metric-space-valued response and the local linear method of Petersen and Müller (2019) can be adopted. Such distance is expected to have the following properties:*

- *The distance ρ on \mathbb{L} coincides with the fiber metric G for any two points on the same fiber. Specifically, for $L_1, L_2 \in \mathbb{L}(p, q)$, $\rho^2(L_1, L_2) = G_{(p,q)}(L_1 - L_2, L_1 - L_2)$.*
- *The distance ρ on the zero section $W_0(p, q) = 0 \in \mathbb{L}(p, q)$ coincides with the geodesic distance on $\mathcal{M} \times \mathcal{M}$. Specifically, for $(p_1, q_1), (p_2, q_2) \in \mathcal{M} \times \mathcal{M}$, $\rho(W_0(p_1, q_1), W_0(p_2, q_2)) = d_{\mathcal{M}^2}((p_1, q_1), (p_2, q_2))$.*
- *When \mathcal{M} is a Euclidean space, especially when $\mathcal{M} = \mathbb{R}$, the estimate derived from Petersen and Müller (2019) under the distance ρ coincides with the classic estimate, i.e., the estimate derived from the same method but applied to the observations $\hat{\mathcal{C}}_{i,jk} \in \mathbb{R}$ that are treated as real-valued responses.*

⁷For the computational purpose, a frame might be adopted, but the resulting estimator is independent of the choice of the frame, since the objective function in (7) does not depend on any frame.

However, such distance ρ does not exist. On one hand, the positive-definiteness of the distance suggests that $\rho(\hat{\mathcal{C}}_{i_1, j_1 k_1}, \hat{\mathcal{C}}_{i_2, j_2 k_2}) \neq 0$ as long as $\hat{\mathcal{C}}_{i_1, j_1 k_1}, \hat{\mathcal{C}}_{i_2, j_2 k_2} \in \mathbb{L}$ reside in different fibers, i.e., when $\hat{\mu}(T_{i_1 j_1}) \neq \hat{\mu}(T_{i_2 j_2})$ or $\hat{\mu}(T_{i_1 k_1}) \neq \hat{\mu}(T_{i_2 k_2})$. On the other hand, when $\mathcal{M} = \mathbb{R}$, the quantities $\hat{\mathcal{C}}_{i_1, j_1 k_1}$ and $\hat{\mathcal{C}}_{i_2, j_2 k_2}$ are treated as real numbers and thus their distance could be zero even when $\hat{\mu}(T_{i_1 j_1}) \neq \hat{\mu}(T_{i_2 j_2})$ or $\hat{\mu}(T_{i_1 k_1}) \neq \hat{\mu}(T_{i_2 k_2})$.

Once an estimate $\hat{\mathcal{C}}$ of the covariance function \mathcal{C} is obtained, according to Theorem 2.1, the intrinsic Riemannian functional principal component proposed in Lin and Yao (2019) can be adopted. Specifically, eigenvalues $\hat{\lambda}_k$ and eigenfunctions $\hat{\psi}_k$ of $\hat{\mathcal{C}}$ can be obtained by eigen-decomposition of $\hat{\mathcal{C}}$, e.g., via the method described in Section 2.3 of Lin and Yao (2019). For estimation of the scores $\xi_{ik} = \langle X_i, \psi_k \rangle$ in the intrinsic Karhunen–Loève expansion $\text{Log}_\mu X_i = \sum_{k=1}^{\infty} \xi_{ik} \psi_k$ proposed in Lin and Yao (2019), numerical approximation to the integral $\langle X_i, \psi_j \rangle$ is infeasible when the data are sparse. In the Euclidean setting, this issue is addressed by the technique of principal analysis through conditional expectation (PACE, Yao et al., 2005). The technique was also adopted by Dai et al. (2020) for their ambient approach to Riemannian functional data analysis on sparsely observed data. To adapt this technique in our intrinsic framework, for each $T_{\hat{\mu}(T_{ij})} \mathcal{M}$, we fix an orthonormal basis $B_{ij,1}, \dots, B_{ij,d}$; in Proposition 3.1 we will show that the computed scores do not depend on the choice of the basis. Then, the observations $\text{Log}_{\hat{\mu}(T_{ij})} Y_{ij}$ and the estimated eigenfunctions $\hat{\psi}_k(T_{ij})$ can be represented by their respective coordinate vectors z_{ij} and $g_{k,ij}$ with respect to the basis. Similarly, the estimated covariance function $\hat{\mathcal{C}}(T_{ij}, T_{il})$ at (T_{ij}, T_{il}) can be represented by a matrix $C_{i,jl}$ of coefficients. By treating the vectors z_{ij} as \mathbb{R}^d -valued observations, the best linear unbiased predictor (BLUP) of ξ_{ik} is given by

$$\hat{\xi}_{ik} = \hat{\lambda}_k g_{k,i}^\top \Sigma_i^{-1} z_i, \quad (8)$$

where $g_{k,i} = (g_{k,i1}^\top, \dots, g_{k,im_i}^\top)^\top$, $z_i = (z_{i1}^\top, \dots, z_{im_i}^\top)^\top$ and

$$\Sigma_i = \hat{\sigma}^2 \mathbf{I} + \begin{pmatrix} C_{i,11} & C_{i,12} & \cdots & C_{i,1m_i} \\ C_{i,21} & C_{i,22} & \cdots & C_{i,2m_i} \\ \vdots & \vdots & \ddots & \vdots \\ C_{i,m_i1} & C_{i,m_i2} & \cdots & C_{i,m_i m_i} \end{pmatrix}$$

with $\hat{\sigma}^2 = \sum_{i=1}^n \sum_{j=1}^{m_i} (ndm_i)^{-1} \text{tr}\{z_{ij} z_{ij}^\top - \hat{\mathcal{C}}(T_{ij}, T_{ij})\}$. The following invariance principle shows that the scores $\hat{\xi}_{ik}$ in (8) are invariant to the choice of bases $B_{ij,1}, \dots, B_{ij,d}$. This extends the invariance principle of Lin and Yao (2019) from the full/dense design to the sparse design.

Proposition 3.1. *The principal component scores $\hat{\xi}_{ik}$ in (8) do not depend on the choice of the orthonormal bases $\{(B_{ij,1}, \dots, B_{ij,d}) : i = 1, \dots, n, j = 1, \dots, m_i\}$.*

4 Asymptotic properties

4.1 Mean function

The pointwise convergence rate of the estimate $\hat{\mu}(t)$ is established in Petersen and Müller (2019), while the uniform convergence rate is derived by Dai et al. (2020). For completeness, we include them here, and establish a new local uniform result that is used in the theoretical analysis of the covariance estimator, as follows. First, we require the following assumptions, where the condition (b) may be replaced with tail and moment conditions on the distributions of Y and X at the cost of much heavier technicalities.

Assumption 4.1.

- (a) The Riemannian manifold \mathcal{M} is complete and simply connected⁸.
- (b) There exists a compact subset of $\mathcal{K} \subset \mathcal{M}$ such that $\Pr\{X(t), Y(t) \in \mathcal{K} \text{ for all } t \in \mathcal{T}\} = 1$.
- (c) The domain \mathcal{T} is a compact interval.
- (d) The probability density function $f(t)$ of T are twice differentiable and satisfies $\inf_{t \in \mathcal{T}} f(t) > 0$.
- (e) The conditional density function $g_y(t)$ of T given Y is twice differentiable and bounded uniformly over $y \in \mathcal{M}$.
- (f) The kernel function K is smooth, symmetric and compactly supported on $[-1, 1]$.

To state the assumption on the regularity of the mean function, we define $u_k(t) := \mathbf{E}\{K_{h_\mu}(T-t)(T-t)^k\}$, $\sigma_0^2(t) := u_0(t)u_2(t) - u_1^2(t)$, and $w(T, t, h_\mu) := \frac{1}{\sigma_0^2(t)}K_{h_\mu}(T-t)[u_2(t) - u_1(t)(T-t)]$. Also, define

$$\tilde{\mu}(t) := \arg \min_{y \in \mathcal{M}} \tilde{Q}_n(y, t), \quad \text{where } \tilde{Q}_n(y, t) := \mathbf{E}\{w(T, t, h_\mu)d_{\mathcal{M}}^2(Y, y)\}.$$

In the above the dependency of $\tilde{Q}_n(y, t)$ and $\tilde{\mu}(t)$ on the sample size n arises from the parameter $h_\mu = h_\mu(n)$. Let $F^*(y, t) = \mathbf{E}d_{\mathcal{M}}^2(Y(t), p)$. The following imposed regularity on the mean function or related quantities is adapted from [Petersen and Müller \(2019\)](#) and is specialized to the Riemannian manifold.

Assumption 4.2.

- (a) The mean curve $\mu(t)$ is twice continuously differentiable. The minimizer $\tilde{\mu}$ exists and is unique.
- (b) For any $\delta > 0$

$$\liminf_{n \rightarrow \infty} \inf_{\substack{d_{\mathcal{M}}(y, \mu(t)) > \delta \\ t \in \mathcal{T}}} \{F^*(y, t) - F^*(\mu(t), t)\} > 0,$$

$$\liminf_{n \rightarrow \infty} \inf_{\substack{d_{\mathcal{M}}(y, \tilde{\mu}(t)) > \delta \\ t \in \mathcal{T}}} \{\tilde{Q}_n(y, t) - \tilde{Q}_n(\tilde{\mu}(t), t)\} > 0.$$

- (c) There exist $\eta_1 > 0$ and $C_1 > 0$ such that for all $t \in \mathcal{T}$ and all y with $d_{\mathcal{M}}(y, \mu(t)) < \eta_1$,

$$\liminf_{n \rightarrow \infty} F^*(y, t) - F^*(\mu(t), t) - C_1 d_{\mathcal{M}}(y, \mu(t))^2 \geq 0.$$

- (d) There exist $\eta_2 > 0$ and $C_2 > 0$ such that for all $t \in \mathcal{T}$ and all y with $d_{\mathcal{M}}(y, \tilde{\mu}(t)) < \eta_2$,

$$\liminf_{n \rightarrow \infty} \tilde{Q}_n(y, t) - \tilde{Q}_n(\tilde{\mu}(t), t) - C_2 d_{\mathcal{M}}(y, \tilde{\mu}(t))^2 \geq 0.$$

The following proposition states the point-wise and uniform convergence rates of the estimated mean function, where the point-wise rate can be derived by extending the proof in [Petersen and Müller \(2019\)](#) and the uniform rate is established in [Dai et al. \(2020\)](#). Note that for a clear exposition, we assume $m_i = m$, while emphasize that extension to more general cases is technically straightforward but notionally complicated ([Zhang and Wang, 2016](#)).

⁸A manifold \mathcal{M} is simply connected if and only if it is path-connected, and for any two continuous paths γ_1 and γ_2 with the same start and end points, γ_1 can be continuously deformed into γ_2 , i.e., there exists a continuous function $\gamma: [0, 1]^2 \rightarrow \mathcal{M}$ such that $\gamma(s, 0) = \gamma_1(s)$ and $\gamma(s, 1) = \gamma_2(s)$ for $s \in [0, 1]$. Here, a manifold is path-connected if for each pair of points there exists a continuous path between them.

Proposition 4.1. *Suppose that Assumptions 2.1, 2.2, 3.1, 4.1 and 4.2 hold. If $h_\mu \rightarrow 0$ and $nmh_\mu \rightarrow \infty$, then for any fixed $t \in \mathcal{T}$,*

$$d_{\mathcal{M}}^2(\mu(t), \hat{\mu}(t)) = O_p\left(h_\mu^4 + \frac{1}{n} + \frac{1}{nmh_\mu}\right).$$

If $h_\mu \rightarrow 0$ and $nmh_\mu/\log n \rightarrow \infty$, then

$$\sup_{t \in \mathcal{T}} d_{\mathcal{M}}^2(\mu(t), \hat{\mu}(t)) = O_p\left(h_\mu^4 + \frac{\log n}{nmh_\mu} + \frac{\log n}{n}\right).$$

To derive the point-wise convergence rate of the estimator $\hat{\mathcal{C}}(s, t)$ in the next subsection, we require a local convergence property of the estimator $\hat{\mu}$. The following Proposition 4.2, which is new in the literature, shows that the local uniform convergence rate is the same as the point-wise rate in Proposition 4.1, and differs from the global uniform convergence rate that has an additional $\log n$ factor. The reason for this phenomenon is that $\mathbf{E}\{K_{h_\mu}(T-t)\} = 1$ at a fixed point t but $\mathbf{E}\{\sup_{t \in \mathcal{T}} K_{h_\mu}(T-t)\} = 1/h_\mu \rightarrow \infty$. Therefore, the additional $\log n$ factor is needed to offset this explosion in the case of global uniform convergence. In the local case, if $h = O(h_\mu)$ and thus $\mathbf{E}\{\sup_{\tau: |\tau-t| \leq h} K_{h_\mu}(T-\tau)\} = O(h/h_\mu) = O(1)$, then no offset is required. The proposition also directly implies the point-wise rate in Proposition 4.1. Its proof can be found in the supplementary material.

Proposition 4.2. *Suppose that Assumptions 2.1, 2.2, 3.1, 4.1 and 4.2 hold. If $h_\mu \rightarrow 0$ and $nmh_\mu \rightarrow \infty$, then for any fixed t and $h = O(h_\mu)$,*

$$\sup_{\tau: |\tau-t| \leq h} d_{\mathcal{M}}^2(\mu(\tau), \hat{\mu}(\tau)) = O_p\left(h_\mu^4 + \frac{1}{n} + \frac{1}{nmh_\mu}\right).$$

4.2 Covariance

To analyze the asymptotic properties of the covariance estimate $\hat{\mathcal{C}}$, we start with the following assumption on the regularity of the covariance function \mathcal{C} . As discussed in Section 2.4, such regularity condition in the manifold setting is made precise and meaningful by the constructed covariance vector bundle \mathbb{L} and the covariant derivative ∇ in (5).

Assumption 4.3. *The covariance function \mathcal{C} is twice differentiable and its second derivatives are continuous.*

To study the asymptotic properties of the estimator $\hat{\mathcal{C}}$, one of the major challenges that are not encountered in the Euclidean setting of Zhang and Wang (2016) or the ambient case of Dai et al. (2020) is to deal with the parallel transport in (7). It turns out that we need to quantify the discrepancy between a tangent vector and the parallelly transported one along a geodesic quadrilateral. We address this issue by the following lemma which might be of independent interest. The proof of the lemma given in the appendix utilizes holonomy theory that seems relatively new in statistics.

Lemma 4.1. *For a compact subset $\mathcal{G} \subset \mathcal{M}$, there exists a constant $c > 0$ depending only on \mathcal{G} , such that for all $p_1, p_2, q_1, q_2, y \in \mathcal{G}$,*

$$\|\mathcal{P}_{q_1}^{p_1} \mathcal{P}_{q_2}^{q_1} \text{Log}_{q_2} y - \mathcal{P}_{p_2}^{p_1} \text{Log}_{p_2} y\|_{p_1} \leq c(d_{\mathcal{M}}(p_1, q_1) + d_{\mathcal{M}}(p_2, q_2)).$$

With the above regularity condition and lemma, the following theorem establishes the point-wise convergence rate of $\hat{\mathcal{C}}$.

Theorem 4.1. *Suppose that Assumptions 2.1, 2.2, 3.1, 4.1, 4.2 and 4.3 hold. If $h_\mu \rightarrow 0$, $h_C = O(h_\mu)$, and $\min\{nmh_\mu, nm^2h_C^2\} \rightarrow \infty$, then for a fixed $t \in \mathcal{T}$,*

$$\left\| \mathcal{P}_{(\hat{\mu}(s), \hat{\mu}(t))}^{(\mu(s), \mu(t))} \hat{\mathcal{C}}(s, t) - \mathcal{C}(s, t) \right\|_{G(\mu(s), \mu(t))}^2 = O_p \left(h_\mu^4 + h_C^4 + \frac{1}{n} + \frac{1}{nmh_\mu} + \frac{1}{nm^2h_C^2} \right). \quad (9)$$

The rate in the above theorem matches the point-wise rate in the Euclidean setting of Zhang and Wang (2016) in the case of $m_1 = \dots = m_n = m$. Unlike Zhang and Wang (2016) who assumed that the mean function is known in their analysis, we do not need such assumption thanks to the local uniform rate of the mean function stated in Proposition 4.2. In our analysis, the local uniform rate can not be replaced with the global uniform rate in Proposition 4.1 without introducing an additional $\log n$ factor. Although the condition $h_C = O(h_\mu)$ is required in order to utilize Proposition 4.2, it does not limit the convergence rate, as a proper choice of h_μ and h_C leads to the following rates that still match the rates of Zhang and Wang (2016).

Corollary 4.1. *Suppose that Assumptions 2.1, 2.2, 3.1, 4.1, 4.2 and 4.3 hold.*

(a) *When $m \asymp n^{1/4}$ or $m \gg n^{1/4}$, with $h_\mu \asymp h_C \asymp n^{-1/4}$, one has*

$$\left\| \mathcal{P}_{(\hat{\mu}(s), \hat{\mu}(t))}^{(\mu(s), \mu(t))} \hat{\mathcal{C}}(s, t) - \mathcal{C}(s, t) \right\|_{G(\mu(s), \mu(t))}^2 = O_p \left(\frac{1}{n} \right).$$

(b) *When $m \ll n^{1/4}$, with $h_\mu \asymp h_C \asymp n^{-1/6}m^{-1/3}$, one has*

$$\left\| \mathcal{P}_{(\hat{\mu}(s), \hat{\mu}(t))}^{(\mu(s), \mu(t))} \hat{\mathcal{C}}(s, t) - \mathcal{C}(s, t) \right\|_{G(\mu(s), \mu(t))}^2 = O_p \left(\frac{1}{n^{2/3}m^{4/3}} \right).$$

Like the Euclidean case, a phase transition is observed at $m \asymp n^{1/4}$. With a proper choice of h_μ and h_C , if m grows at least as fast as $n^{1/4}$, it does not impact the convergence rate. Otherwise, the sampling rate m becomes an integrable part of the convergence rate of $\hat{\mathcal{C}}$. In particular, when $m \ll n^{1/4}$, the choice $h_\mu \asymp n^{-1/6}m^{-1/3}$ is required to respect the condition $h_C = O(h_\mu)$. This choice is strictly larger than the optimal choice $h_\mu \asymp (nm)^{-1/5}$ that is implied by Proposition 4.1 in the case of $m \ll n^{1/4}$. This suggests that oversmoothing in the mean function estimation is required in order to reach the optimal point-wise rate of the covariance estimator when $m \ll n^{1/4}$.

The following results establish the uniform convergence rate of the covariance estimator $\hat{\mathcal{C}}$.

Theorem 4.2. *Suppose that Assumptions 2.1, 2.2, 3.1, 4.1, 4.2 and 4.3 hold. If $h_\mu \rightarrow 0$, $nmh_\mu/\log n \rightarrow \infty$ and $nm^2h_C^2/\log n \rightarrow \infty$, then*

$$\sup_{(s, t) \in \mathcal{T}^2} \left\| \mathcal{P}_{(\hat{\mu}(s), \hat{\mu}(t))}^{(\mu(s), \mu(t))} \hat{\mathcal{C}}(s, t) - \mathcal{C}(s, t) \right\|_{G(\mu(s), \mu(t))}^2 = O_p \left(h_\mu^4 + h_C^4 + \frac{\log n}{n} + \frac{\log n}{nmh_\mu} + \frac{\log n}{nm^2h_C^2} \right). \quad (10)$$

Corollary 4.2. *Suppose that Assumptions 2.1, 2.2, 3.1, 4.1, 4.2 and 4.3 hold.*

(a) *When $m \asymp n^{1/4}$ or $m \gg n^{1/4}$, with $h_\mu \asymp h_C \asymp n^{-1/4}$, one has*

$$\sup_{(s, t) \in \mathcal{T}^2} \left\| \mathcal{P}_{(\hat{\mu}(s), \hat{\mu}(t))}^{(\mu(s), \mu(t))} \hat{\mathcal{C}}(s, t) - \mathcal{C}(s, t) \right\|_{G(\mu(s), \mu(t))}^2 = O_p \left(\frac{\log n}{n} \right).$$

(b) When $m \ll n^{1/4}$, with $h_\mu \asymp n^{-1/5} m^{-1/5} (\log n)^{1/5}$ and $h_C \asymp n^{-1/6} m^{-1/3} (\log n)^{1/6}$, one has

$$\sup_{(s,t) \in \mathcal{T}^2} \left\| \mathcal{P}_{(\hat{\mu}(s), \hat{\mu}(t))}^{\mu(s), \mu(t)} \hat{C}(s, t) - C(s, t) \right\|_{G(\mu(s), \mu(t))}^2 = O_p \left(\frac{(\log n)^{2/3}}{n^{2/3} m^{4/3}} \right).$$

The rates in the above again match the uniform rates of [Zhang and Wang \(2016\)](#). It also coincides with the rate⁹ in [Dai and Müller \(2018\)](#). It is interesting to see that, when $m \ll n^{1/4}$, the choice of h_μ in the corollary is the same as the optimal choice implied by [Proposition 4.1](#), which suggests that no oversmoothing is needed in order to reach the optimal uniform rate for the covariance estimator \hat{C} . This is because, the local uniform result of [Proposition 4.2](#) and thus the condition $h_C = O(h_\mu)$ are not required, as the role of [Proposition 4.2](#) in the analysis is now played by [Proposition 4.1](#).

5 Simulation studies

We consider three different manifolds for illustrating the numerical properties of the proposed covariance estimator (7) in [Section 3](#); the numerical performance of the mean estimator can be found in [Dai et al. \(2020\)](#). Namely, they are the two-dimensional unit sphere \mathbb{S}^2 , the manifold Sym_{LC}^+ of symmetric positive-definite 2×2 matrices with the Log-Cholesky metric ([Lin, 2019](#)), and the manifold Sym_{AF}^+ of symmetric positive-definite 2×2 matrices with the affine-invariant metric ([Moakher, 2005](#)), representing manifolds of positive, zero and negative sectional curvature, respectively. Note that although Sym_{LC}^+ and Sym_{AF}^+ share the same collection of matrices, they are endowed with different Riemannian metric tensors and thus have fundamentally different Riemannian geometry. We set $\mathcal{T} = [0, 1]$. The sampling rate m_i is randomly sampled from $\text{Poisson}(m) + 2$, where $\text{Poisson}(m)$ is a Poisson distribution with parameter m . Conditional on m_i , T_{i1}, \dots, T_{im_i} are i.i.d. sampled from the uniform distribution $\text{Uniform}(0, 1)$. The random process X and its mean and covariance functions are described below.

Sphere \mathbb{S}^2 . We parameterize $\mathbb{S}^2 = \{(x, y, z) \in \mathbb{R}^3 : x^2 + y^2 + z^2 = 1\}$ by the polar coordinate system

$$\begin{aligned} x(u, v) &= \cos(u) \\ y(u, v) &= \sin(u) \cos(v) \\ z(u, v) &= \sin(u) \sin(v) \end{aligned}$$

for $u \in [0, \pi]$ and $v \in [0, 2\pi)$. This coordinate system also gives rise to a local chart $\phi : U \rightarrow [0, \pi) \times [0, 2\pi)$ on $U = \mathbb{S}^2 \setminus \{(-1, 0, 0)\}$. Let $B_1(t) = \frac{\partial \phi}{\partial u}|_{\mu(t)}$ and $B_2(t) = \frac{\partial \phi}{\partial v}|_{\mu(t)}$. The random process X is then given by

$$X(t) = \text{Exp}_{\mu(t)}(tZ_1 B_1(t) + tZ_2 B_2(t))$$

with $Z_1, Z_2 \stackrel{i.i.d.}{\sim} \text{Uniform}(-0.1, 0.1)$. The mean curve μ of X is $\mu(t) = (u(t), v(t)) = (0, \pi t/2)$ in the above polar coordinate. The covariance function is $C(s, t) = \frac{st}{300} \mathbf{I}_2$ under the frame (B_1, B_2) , where \mathbf{I}_2 denotes the 2×2 identity matrix. The contaminated observations are

$$Y_{ij} = \text{Exp}_{\mu(T_{ij})} \{ (T_{ij} Z_{1i} + \varepsilon_{ij}) B_1(T_{ij}) + (T_{ij} Z_{2i} + \varepsilon_{ij}) B_2(T_{ij}) \},$$

⁹Note that the extra term $1/(nmh_C)$ in [Dai and Müller \(2018\)](#) is dominated by $1/n + 1/(nm^2 h_C^2)$ due to the inequality of arithmetic and geometric means, i.e., $\sqrt{ab} \leq (a+b)/2$.

where $Z_{1i}, Z_{2i} \stackrel{i.i.d.}{\sim} \text{Uniform}(-0.1, 0.1)$, and $\varepsilon_{ij} \stackrel{i.i.d.}{\sim} \text{Uniform}(-a, a)$ with a chosen to make $\text{SNR} = 5$ defined by

$$\text{SNR} := \frac{\mathbf{E} \int_{\mathcal{T}} \|\text{Log}_{\mu(t)} X(t)\|_{\mu(t)}^2 dt}{\mathbf{E} \int_{\mathcal{T}} \|\varepsilon(t)\|_{\mu(t)}^2 dt}. \quad (11)$$

Manifold Sym_{LC}^+ . The population X is set to be

$$X(t) = \begin{pmatrix} e^{t+tZ_1} & 0 \\ t+tZ_3 & e^{t+tZ_2} \end{pmatrix} \begin{pmatrix} e^{t+tZ_1} & t+tZ_3 \\ 0 & e^{t+tZ_2} \end{pmatrix} \quad \text{with } Z_1, Z_2 \stackrel{i.i.d.}{\sim} \text{Uniform}(-0.1, 0.1).$$

The mean μ is a geodesic with $\mu(0) = \mathbf{I}_2$ and the covariance $\mathcal{C}(s, t)$ can be represented as a 3×3 matrix if a coordinate frame is fixed. The contaminated observations are

$$Y_{ij} = \begin{pmatrix} e^{T_{ij}+T_{ij}Z_{1i}+\varepsilon_{ij}} & 0 \\ T_{ij} + T_{ij}Z_{3i} + \varepsilon_{ij} & e^{T_{ij}+T_{ij}Z_{2i}+\varepsilon_{ij}} \end{pmatrix} \begin{pmatrix} e^{T_{ij}+T_{ij}Z_{1i}+\varepsilon_{ij}} & T_{ij} + T_{ij}Z_{3i} + \varepsilon_{ij} \\ 0 & e^{T_{ij}+T_{ij}Z_{2i}+\varepsilon_{ij}} \end{pmatrix}$$

where $Z_{1,i}, Z_{2,i}, Z_{3,i} \stackrel{i.i.d.}{\sim} \text{Uniform}(-0.1, 0.1)$ and $\varepsilon_{ij} \stackrel{i.i.d.}{\sim} \text{Uniform}(-a, a)$ with a set to satisfy $\text{SNR} = 5$ defined in (11).

Manifold Sym_{AF}^+ . The random process $X(t)$ is set to

$$X(t) = \begin{pmatrix} \frac{1}{4}e^{t+tZ_1} + \frac{3}{4}e^{t+tZ_2} & \frac{\sqrt{3}}{4}e^{t+tZ_1} - \frac{\sqrt{3}}{4}e^{t+tZ_2} \\ \frac{\sqrt{3}}{4}e^{t+tZ_1} - \frac{\sqrt{3}}{4}e^{t+tZ_2} & \frac{3}{4}e^{t+tZ_1} + \frac{1}{4}e^{t+tZ_2} \end{pmatrix},$$

for $Z_1, Z_2 \stackrel{i.i.d.}{\sim} \text{Uniform}(-0.1, 0.1)$. The mean $\mu(t)$ is a geodesic starting at \mathbf{I}_2 , and the covariance $\mathcal{C}(s, t) = \mathbf{E}\{\text{Log}_{\mu(s)} X(s) \otimes \text{Log}_{\mu(t)} X(t)\}$ can be represented as a 3×3 matrix if a coordinate frame is fixed. The contaminated observations are

$$Y_{ij} = \begin{pmatrix} \frac{1}{4}e^{T_{ij}+T_{ij}Z_{1i}+\varepsilon_{ij}} + \frac{3}{4}e^{T_{ij}+T_{ij}Z_{2i}+\varepsilon_{ij}} & \frac{\sqrt{3}}{4}e^{T_{ij}+T_{ij}Z_{1i}+\varepsilon_{ij}} - \frac{\sqrt{3}}{4}e^{T_{ij}+T_{ij}Z_{2i}+\varepsilon_{ij}} \\ \frac{\sqrt{3}}{4}e^{T_{ij}+T_{ij}Z_{1i}+\varepsilon_{ij}} - \frac{\sqrt{3}}{4}e^{T_{ij}+T_{ij}Z_{2i}+\varepsilon_{ij}} & \frac{3}{4}e^{T_{ij}+T_{ij}Z_{1i}+\varepsilon_{ij}} + \frac{1}{4}e^{T_{ij}+T_{ij}Z_{2i}+\varepsilon_{ij}} \end{pmatrix},$$

where $Z_{1i}, Z_{2i} \stackrel{i.i.d.}{\sim} \text{Uniform}(-0.1, 0.1)$ and $\varepsilon_{ij} \stackrel{i.i.d.}{\sim} \text{Uniform}(-a, a)$ with a set to satisfy $\text{SNR} = 5$ defined in (11).

We consider different sample sizes and sampling rates, namely, $n = 100, 200, 400$ and $m = 5, 10, 20, 30$. Each simulation is repeated independently 100 times. The bandwidths h_μ and h_C are selected by GCV proposed in Dai et al. (2020). Estimation quality is measured by relative mean uniform integrated error (rMUIE) and relative root mean integrated squared error (rRMISE), defined by

$$\begin{aligned} \text{rMUIE} &:= \frac{\mathbf{E} \sup_{s, t \in \mathcal{T}} \|\mathcal{P}_{(\hat{\mu}(s), \hat{\mu}(t))}^{(\mu(s), \mu(t))} \hat{\mathcal{C}}(s, t) - \mathcal{C}(s, t)\|_G}{\sup_{s, t \in \mathcal{T}} \|\mathcal{C}(s, t)\|_G}, \\ \text{rRMISE} &:= \frac{\{\mathbf{E} \int_{\mathcal{T}^2} \|\mathcal{P}_{(\hat{\mu}(s), \hat{\mu}(t))}^{(\mu(s), \mu(t))} \hat{\mathcal{C}}(s, t) - \mathcal{C}(s, t)\|_G^2 ds dt\}^{1/2}}{\{\int_{\mathcal{T}^2} \|\mathcal{C}(s, t)\|_G^2\}^{1/2}}. \end{aligned} \quad (12)$$

Table 1: rMUIE and its Monte Carlo standard errors under different settings

manifold	n	rMUIE			
		$m = 5$	$m = 10$	$m = 20$	$m = 30$
\mathbb{S}^2	100	23.46(9.98)	21.01(8.60)	18.48(6.35)	18.12(6.32)
	200	18.23(7.22)	16.68(6.04)	15.08(4.86)	14.01(4.37)
	400	15.21(4.14)	13.64(4.45)	12.29(3.37)	11.79(3.31)
Sym_{LC}^+	100	29.94(14.75)	26.09(9.62)	22.50(5.78)	22.45(6.85)
	200	22.85(7.04)	20.37(7.07)	17.44(5.39)	16.44(4.02)
	400	17.69(7.74)	15.37(3.84)	13.94(3.05)	13.60(2.61)
Sym_{AF}^+	100	25.26(13.02)	22.18(11.07)	20.31(8.00)	18.15(5.95)
	200	20.15(8.86)	17.14(6.61)	14.09(5.00)	13.49(4.83)
	400	15.82(7.03)	14.39(5.66)	12.74(4.37)	12.61(3.55)

Table 2: rRMISE and its Monte Carlo standard errors under different settings

manifold	n	rRMISE			
		$m = 5$	$m = 10$	$m = 20$	$m = 30$
\mathbb{S}^2	100	20.95(2.15)	19.36(2.50)	16.95(1.67)	16.94(1.97)
	200	16.33(1.56)	15.34(1.51)	14.28(1.19)	13.20(1.43)
	400	13.82(1.12)	12.80(1.19)	11.22(1.02)	10.97(1.10)
Sym_{LC}^+	100	26.32(2.42)	23.33(1.98)	21.20(1.57)	20.98(1.71)
	200	20.76(1.58)	17.92(1.39)	16.56(1.15)	16.12(1.02)
	400	16.20(1.15)	14.37(0.90)	13.55(0.82)	13.18(0.93)
Sym_{LC}^+	100	20.96(2.42)	18.97(1.95)	18.84(1.92)	17.58(1.72)
	200	16.67(1.61)	15.23(1.21)	13.22(1.35)	12.70(1.29)
	400	13.20(1.19)	12.87(1.22)	11.17(0.98)	10.84(1.00)

The results, summarized in Tables 1 and 2, show that the estimation errors in terms of both rMUIE and rRMISE decrease as n or m increases, and thus demonstrate the effectiveness of the proposed estimation method. A phase transition phenomenon is also observed: When m is increased from 5 to 10 or 20, the errors in terms of both rMUIE and rRMISE decrease substantially, while when m is further increased to 30, the decrease in errors is marginal. This phenomenon, predicted by our theoretical analysis in Section 4, suggests that for a fixed sample size, when $m = 5$ or $m = 10$ the errors are primarily due to the low sampling rate m , while when $m = 30$ or higher the errors are mainly contributed by the limited sample size.

6 Application to longitudinal diffusion tensors

We apply the proposed framework to analyze longitudinal diffusion tensors from Alzheimer’s Disease Neuroimaging Initiative¹⁰ (ADNI). Diffusion tensor imaging (DTI), a special kind of diffusion-weighted magnetic resonance imaging, has been extensively adopted in brain science to investigate white matter tractography. In a DTI image, each brain voxel is associated with a 3×3 symmetric positive-definite matrix, called diffusion tensor, that characterizes diffusion of water molecules in the voxel. As diffusion of water molecules carries rich information about axons, diffusion tensor imaging has important applications in both clinical diagnostics

¹⁰<http://adni.loni.usc.edu/>

and scientific research related to brain diseases. From a statistical perspective, diffusion tensors are modeled as random elements in $\text{Sym}_*^+(3)$, and have been studied extensively, such as Fillard et al. (2005); Arsigny et al. (2006); Lenglet et al. (2006); Pennec et al. (2006); Fletcher and Joshi (2007); Dryden et al. (2009); Zhu et al. (2009); Pennec (2020), among many others. In these works $\text{Sym}_*^+(3)$ is endowed with a Riemannian metric or a non-Euclidean distance that aims to alleviate or completely eliminate swelling effect (Arsigny et al., 2007). However, none of them consider the longitudinal aspect of diffusion tensors.

We focus on the hippocampus, a brain region that plays an important role in memory and is central to Alzheimer’s disease (Lindberg et al., 2012), and only include in the study subjects with at least four properly recorded DTI images. This results in a sample of $n = 177$ subjects with age ranging from 55.2 to 93.5. Among them, 42 subjects are cognitively normal (CN), while the others (AD) developed one of early mild cognitive impairment, mild cognitive impairment, late mild cognitive impairment and Alzheimer’s disease. On average, there are $m = 5.5$ DTI scans for each subject, which shows that the data are rather sparsely recorded. A standard procedure that includes denoising, eddy current and motion correction, skull stripping, bias correction and normalization is adopted to preprocess the raw images. Based on the preprocessed DTI images, diffusion tensors are derived. We endow $\text{Sym}_*^+(3)$ with the Log-Cholesky metric (Lin, 2019) and turn it into a Riemannian manifold of nonpositive sectional curvature. Under the Log-Cholesky framework that avoids swelling effect and meanwhile enjoys computational efficiency, the Fréchet mean of the tensors inside hippocampus is calculated for each DTI scan, which represents a coarse-grain summary of hippocampal diffusion tensors. As we shall see below, this averaged mean tensor is already capable of illuminating some differences of the diffusion dynamics between the AD and CN groups.

For the Fréchet mean trajectories, the selected bandwidths via leave-one-out cross-validation are 4.2 and 5.7 for the AD and CN groups, respectively. The resulting trajectories, depicted in Figure 7, where each tensor is visualized as an ellipsoid whose volume corresponds to the determinant of the tensor, suggest that, overall the averaged hippocampal diffusion tensor remains rather stable for the CN group; the tensors at age 55.2 and 93.5 that markedly depart from the others could be due to boundary effect, i.e., there are relatively less data around the two boundary time points. In contrast, for the AD group, the dynamic tensor varies more substantially, and the diffusion (measured by the determinant of tensors and indicated by volume of ellipsoids) seems larger. Also, the mean trajectory of the AD group exhibits slightly lower fractional anisotropy at each time point. Fractional anisotropy, defined for each 3×3 symmetric positive-definite matrix A by

$$\text{FA} = \sqrt{\frac{3}{2} \frac{(\rho_1 - \bar{\rho})^2 + (\rho_2 - \bar{\rho})^2 + (\rho_3 - \bar{\rho})^2}{\rho_1^2 + \rho_2^2 + \rho_3^2}}$$

where ρ_1, ρ_2, ρ_3 are eigenvalues of A and $\bar{\rho} = (\rho_1 + \rho_2 + \rho_3)/3$, describes the degree of anisotropy of diffusion of water molecules. It is close to zero unless movement of the water molecules is constrained by structures such as white matter fibers. The below-normal fractional anisotropy might then suggest some damage on the hippocampal structure for the AD group.

For the covariance function, the selected bandwidth is 3.5 for the AD group and 4.5 for the CN group. Shown in Figure 8 are the first three intrinsic Riemannian functional principal components that are mapped on $\text{Sym}_*^+(3)$ via the Riemannian exponential maps $\text{Exp}_{\hat{\mu}(t)}$. They respectively account for 40.2%, 22.2% and 7.0% of variance for the AD group, and 40.7%, 19.4% and 8.0% of variance for the CN group. These components, compared side by side in Figure 8, exhibit different patterns between the two cohorts. For instance, the Riemannian functional principal components of the AD group show relatively larger diffusion and more dynamics over time. In addition, they exhibit relatively lower fractional anisotropy, which suggests that individual diffusion tensor trajectories in the AD group tend to deviate from their mean trajectory along the direction with below-normal fractional anisotropy.

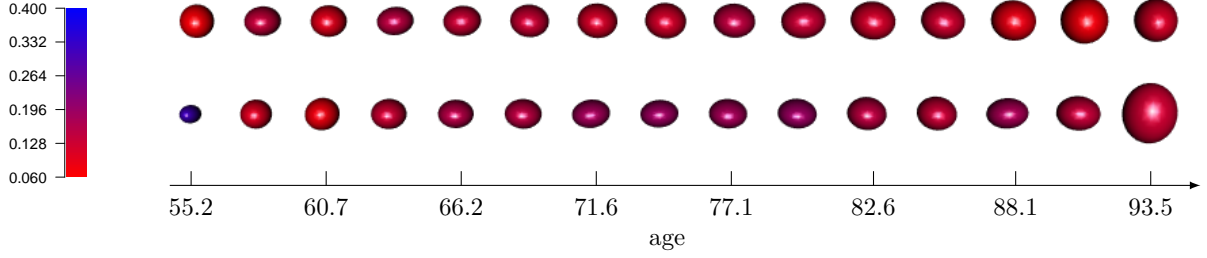


Figure 7: Mean functions. Top: AD group; bottom: CN group. The color encodes fractional anisotropy.

In summary, via the proposed framework we find that there are differences in longitudinal development of hippocampus between cognitively normal subjects and patients with Alzheimer’s disease. In the above analysis, the averaged hippocampal diffusion tensors do not capture the rich spatial information of all tensors within the hippocampus. To account for such information, all hippocampal diffusion tensors shall be taken into consideration by being modeled as an $\text{Sym}_*^+(3)$ -valued function defined on the hippocampal region which is a three-dimensional domain of \mathbb{R}^3 . Along with the temporal dynamics, for each subject there are spatiotemporal Riemannian manifold-valued data, with the sparseness along the temporal direction. Our framework can be extended to analyze such data, but the extension requires substantial development and is left for future study.

A Proofs

Proof of Theorem 2.1. According to the definition of $\mathcal{C}(s, t)$, for any $u, v \in \mathcal{T}(\mu)$, we have

$$\begin{aligned}
\langle\langle \int_{\mathcal{T}} \mathcal{C}(s, \cdot) u(s) ds, v \rangle\rangle_{\mu} &= \int_{\mathcal{T}} \int_{\mathcal{T}} \langle \mathcal{C}(s, t) u(s), v(t) \rangle_{\mu(t)} ds dt \\
&= \int_{\mathcal{T}} \int_{\mathcal{T}} \mathbf{E} \{ \langle \text{Log}_{\mu(s)} X(s), u(s) \rangle_{\mu(s)} \langle \text{Log}_{\mu(t)} X(t), v(t) \rangle_{\mu(t)} \} ds dt \\
&= \mathbf{E} \left\{ \int_{\mathcal{T}} \langle \text{Log}_{\mu(s)} X(s), u(s) \rangle_{\mu(s)} ds \int_{\mathcal{T}} \langle \text{Log}_{\mu(t)} X(t), v(t) \rangle_{\mu(t)} dt \right\} \\
&= \mathbf{E} (\langle \text{Log}_{\mu} X, u \rangle_{\mu} \langle \text{Log}_{\mu} X, v \rangle_{\mu}) \\
&= \langle\langle \mathbf{C}u, v \rangle\rangle_{\mu}.
\end{aligned}$$

According to Riesz representation theory, $(\mathbf{C}u)(t) = \int_{\mathcal{T}} \mathcal{C}(s, t) u(s) ds$. \square

Proof of Theorem 2.2. To see that $\{(\pi^{-1}(U_{\alpha} \times U_{\beta}), \varphi_{\alpha, \beta}) : (\alpha, \beta) \in \mathcal{J}^2\}$ is a smooth atlas, it is sufficient to check the smoothness of the transition maps. Suppose that $(p, q, \sum_{j,k=1}^d v_{jk} B_{\alpha, j}(p) \otimes B_{\beta, k}(q)) \in \pi^{-1}(U_{\alpha} \times U_{\beta}) \cap \pi^{-1}(U_{\tilde{\alpha}} \times U_{\tilde{\beta}})$ is also represented by $(p, q, \sum_{j,k=1}^d \tilde{v}_{jk} B_{\tilde{\alpha}, j}(p) \otimes B_{\tilde{\beta}, k}(q))$. The transformation from the coefficient vector $v = (v_{11}, v_{12}, \dots, v_{dd})$ to $\tilde{v} = (\tilde{v}_{11}, \tilde{v}_{12}, \dots, \tilde{v}_{dd})$ is smooth, since $\tilde{v} = \{\mathcal{J}_{\alpha}^{\top}(p) \otimes \mathcal{J}_{\beta}^{\top}(q)\} v$ and $\mathcal{J}_{\alpha}^{\top}(p)$, $\mathcal{J}_{\beta}^{\top}(q)$ and their Kronecker product $\mathcal{J}_{\alpha}^{\top}(p) \otimes \mathcal{J}_{\beta}^{\top}(q)$ are respectively smooth in p , q and (p, q) , where $\mathcal{J}_{\alpha}(\cdot)$ denotes the Jacobian matrix that transforms the basis $\{B_{\alpha, 1}(\cdot), \dots, B_{\alpha, d}(\cdot)\}$ into $\{B_{\tilde{\alpha}, 1}(\cdot), \dots, B_{\tilde{\alpha}, d}(\cdot)\}$.

According to the vector bundle construction lemma (Lemma 5.5, Lee, 2002), it is sufficient to check that when $U := (U_{\alpha} \times U_{\beta}) \cap (U_{\tilde{\alpha}} \times U_{\tilde{\beta}}) \neq \emptyset$ for some indices $\alpha, \beta, \tilde{\alpha}, \tilde{\beta}$, the composite map $\Phi_{\alpha, \beta} \circ \Phi_{\tilde{\alpha}, \tilde{\beta}}^{-1}$ from $U \times \mathbb{R}^{d^2}$ to itself has the form $\Phi_{\alpha, \beta} \circ \Phi_{\tilde{\alpha}, \tilde{\beta}}^{-1} = (p, q, \mathcal{J}(p, q)v)$ for a smooth map $\mathcal{J} : U \rightarrow \text{GL}(d^2, \mathbb{R})$, where $\text{GL}(d^2, \mathbb{R})$ is the collection of invertible real $d^2 \times d^2$ matrices. From above discussion, we have $\mathcal{J}(p, q) = \mathcal{J}_{\alpha}^{\top}(p) \otimes \mathcal{J}_{\beta}^{\top}(q)$ is smooth in (p, q) . In addition, $\mathcal{J}(p, q) \in \text{GL}(d^2, \mathbb{R})$ since both $\mathcal{J}_{\alpha}^{\top}(p)$ and $\mathcal{J}_{\beta}^{\top}(q)$ are invertible and so is their

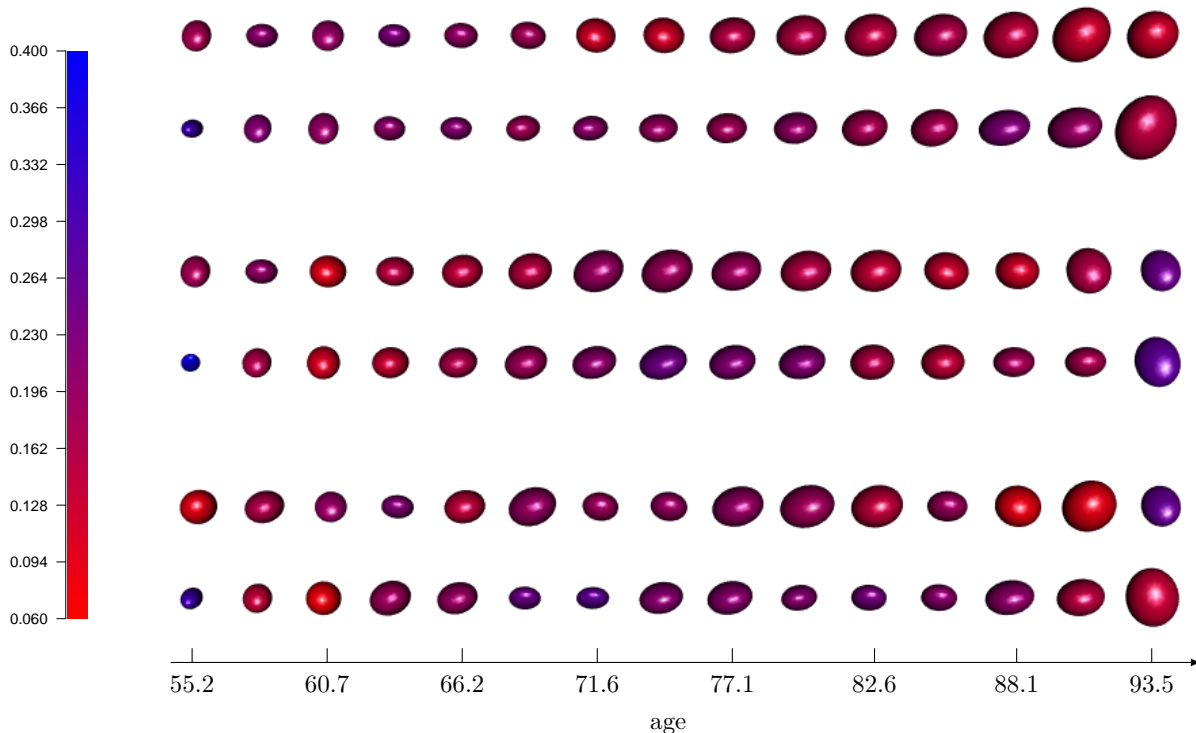


Figure 8: The first principal component of AD group (Row 1) and CN group (Row 2), the second principal component of AD group (Row 3) and CN group (Row 4), and the third principal component of AD group (Row 5) and CN group (Row 6). The color encodes fractional anisotropy.

Kronecker product. Note that the vector bundle construction lemma also asserts that any compatible atlas for \mathcal{M} gives rise to the same smooth structure on \mathbb{L} . \square

Proof of Theorem 2.3. One can show that the parallel transport defined in (4) is a genuine parallel transport satisfying the property of Definition A.54 of Rodrigues and Capelas de Oliveira (2016) on the vector bundle. Then the conclusion directly follows from Definitions A.55 and A.57 of Rodrigues and Capelas de Oliveira (2016) and the remarks right below them. \square

Proof of Theorem 2.4. We first show that the definition (6) is invariant to the choice of orthonormal bases. To this end, fix an orthonormal basis in $T_q\mathcal{M}$, and suppose that $\{\tilde{e}_1, \dots, \tilde{e}_d\}$ is another orthonormal basis in $T_p\mathcal{M}$ and is related to $\{e_1, \dots, e_d\}$ by a $d \times d$ unitary matrix \mathbf{O} . Let A_1 and A_2 be the respective matrix representation of L_1 and L_2 under the basis $\{e_1, \dots, e_d\}$. Then their matrix representation under the basis $\{\tilde{e}_1, \dots, \tilde{e}_d\}$ is $\tilde{A}_1 = \mathbf{O}A_1$ and $\tilde{A}_2 = \mathbf{O}A_2$, respectively. The inner product $G_{p,q}(L_1, L_2)$ is then calculated by $\text{tr}(\tilde{A}_1^\top \tilde{A}_2) = \text{tr}(A_1^\top \mathbf{O}^\top \mathbf{O} A_2) = \text{tr}(A_1^\top A_2)$, which shows that $G_{p,q}(L_1, L_2)$ is invariant to the choice of bases in $T_p\mathcal{M}$. Its invariance to the choice of bases in $T_q\mathcal{M}$ can be proved in a similar fashion.

The smoothness of G can be established by an argument similar to the one leading to Theorem 2.2 in conjunction with smoothness of the trace of matrices. To see that the parallel transport (4) preserves the bundle metric and thus defines isometries among fibers of \mathbb{L} , i.e., for any $L_1, L_2 \in \mathbb{L}(p_1, q_1)$,

$$G_{(p_1, q_1)}(L_1, L_2) = G_{(p_2, q_2)}(\mathcal{P}_{(p_1, q_1)}^{(p_2, q_2)} L_1, \mathcal{P}_{(p_1, q_1)}^{(p_2, q_2)} L_2),$$

suppose that $\{e_1, \dots, e_d\}$ is an orthogonal basis of $T_{p_1}\mathcal{M}$. Then $\{\mathcal{P}_{p_1}^{p_2} e_1, \dots, \mathcal{P}_{p_1}^{p_2} e_d\}$ is an orthogonal basis of

$T_{p_2}\mathcal{M}$. Therefore,

$$\begin{aligned} G_{(p_2, q_2)}(\mathcal{P}_{(p_1, q_1)}^{(p_2, q_2)} L_1, \mathcal{P}_{(p_1, q_1)}^{(p_2, q_2)} L_2) &= \sum_{k=1}^d \langle (\mathcal{P}_{(p_1, q_1)}^{(p_2, q_2)} L_1)(\mathcal{P}_{p_1}^{p_2} e_k), (\mathcal{P}_{(p_1, q_1)}^{(p_2, q_2)} L_2)(\mathcal{P}_{p_1}^{p_2} e_k) \rangle_{q_2} \\ &= \sum_{k=1}^d \langle \mathcal{P}_{q_1}^{q_2} [L_1(e_k)], \mathcal{P}_{q_1}^{q_2} [L_2(e_k)] \rangle_{q_2} \\ &= \sum_{k=1}^d \langle L_1(e_k), L_2(e_k) \rangle_{q_1} = G_{(p_1, q_1)}(L_1, L_2), \end{aligned}$$

which completes the proof. \square

Proof of Proposition 3.1. Suppose that $(\tilde{B}_{ij,1}, \dots, \tilde{B}_{ij,d})$ is another orthonormal basis for $T_{\hat{\mu}(T_{ij})}\mathcal{M}$, and \mathbf{O}_{ij} is the unitary matrix that relates $(B_{ij,1}, \dots, B_{ij,d})$ to $(\tilde{B}_{ij,1}, \dots, \tilde{B}_{ij,d})$. Then the coefficient vectors \tilde{z}_{ij} and $\tilde{g}_{k,ij}$ of $\text{Log}_{\hat{\mu}(T_{ij})} Y_{ij}$ and $\hat{\psi}_k(T_{ij})$ under the basis $(\tilde{B}_{ij,1}, \dots, \tilde{B}_{ij,d})$ are linked to z_{ij} and $g_{k,ij}$ by $\tilde{z}_{ij} = \mathbf{O}_{ij} z_{ij}$ and $\tilde{g}_{k,ij} = \mathbf{O}_{ij} g_{k,ij}$, respectively. Similarly, $\tilde{C}_{i,jl}$ is linked to $C_{i,jl}$ by $\tilde{C}_{i,jl} = \mathbf{O}_{ij} C_{i,jl} \mathbf{O}_{il}^\top$. More concisely, if we put

$$\mathbf{O}_i = \begin{pmatrix} \mathbf{O}_{i1} & & & \\ & \mathbf{O}_{i2} & & \\ & & \ddots & \\ & & & \mathbf{O}_{im_i} \end{pmatrix},$$

then $\tilde{z}_i = \mathbf{O}_i z_i$, $\tilde{g}_{k,i} = \mathbf{O}_i g_{k,i}$ and $\tilde{\Sigma}_i = \mathbf{O}_i \Sigma_i \mathbf{O}_i^\top$, which are the counterpart of z_i , $g_{k,i}$ and Σ_i under the bases $(\tilde{B}_{ij,1}, \dots, \tilde{B}_{ij,d})$, respectively. Note that $\tilde{\Sigma}_i^{-1} = (\mathbf{O}_i \Sigma_i \mathbf{O}_i^\top)^{-1} = \mathbf{O}_i^{-\top} \Sigma_i^{-1} \mathbf{O}_i^{-1} = \mathbf{O}_i \Sigma_i^{-1} \mathbf{O}_i^\top$ since \mathbf{O}_{ij} are unitary matrices and thus $\mathbf{O}_i^{-1} = \mathbf{O}_i^\top$. Now we see that $\tilde{g}_{k,i}^\top \tilde{\Sigma}_i^{-1} \tilde{z}_i = g_{k,i}^\top \mathbf{O}_i^\top \mathbf{O}_i \Sigma_i^{-1} \mathbf{O}_i \mathbf{O}_i^\top z_i = g_{k,i}^\top \Sigma_i^{-1} z_i$, which clearly implies that the scores $\hat{\xi}_{ik}$ calculated under the bases $(\tilde{B}_{ij,1}, \dots, \tilde{B}_{ij,d})$ is identical to the one computed under the bases $(B_{ij,1}, \dots, B_{ij,d})$. \square

Proof of Lemma 4.1. Notice that

$$\begin{aligned} & \| \mathcal{P}_{q_1}^{p_1} \mathcal{P}_{q_2}^{q_1} \text{Log}_{q_2} y - \mathcal{P}_{p_2}^{p_1} \text{Log}_{p_2} y \|_{p_1} \\ &= \| \mathcal{P}_{p_2}^{q_2} \mathcal{P}_{p_1}^{p_2} \mathcal{P}_{q_1}^{p_1} \mathcal{P}_{q_2}^{q_1} \text{Log}_{q_2} y - \mathcal{P}_{p_2}^{q_2} \text{Log}_{p_2} y \|_{q_2} \\ &\leq \| \mathcal{P}_{p_2}^{q_2} \mathcal{P}_{p_1}^{p_2} \mathcal{P}_{q_1}^{p_1} \mathcal{P}_{q_2}^{q_1} \text{Log}_{q_2} y - \text{Log}_{q_2} y \|_{q_2} + \| \text{Log}_{q_2} y - \mathcal{P}_{p_2}^{q_2} \text{Log}_{p_2} y \|_{q_2}, \end{aligned}$$

where the equality follows from the fact that parallel transport preserves the inner product. Note that the operator $\mathcal{P}_{p_2}^{q_2} \mathcal{P}_{p_1}^{p_2} \mathcal{P}_{q_1}^{p_1} \mathcal{P}_{q_2}^{q_1}$ moves a tangent vector parallelly along a geodesic quadrilateral defined by the the points p_1, p_2, q_1, q_2 . The holonomy theory (Eq (6), Nichols et al., 2016) and the compactness of \mathcal{G} suggests that there exists a constant $c_1 > 0$ depending only on \mathcal{G} , such that for any $v \in T_{q_2}\mathcal{M}$ with $\|v\|_{q_2} \leq \text{diam}(\mathcal{G})$,

$$\begin{aligned} & \| \mathcal{P}_{p_2}^{q_2} \mathcal{P}_{p_1}^{p_2} \mathcal{P}_{q_2}^{q_1} v - v \|_{q_2} \leq c_1 \| \text{Log}_{q_2} p_2 \|_{q_2} = c_1 d_{\mathcal{M}}(p_2, q_2), \\ & \| \mathcal{P}_{p_1}^{q_2} \mathcal{P}_{q_1}^{p_1} \mathcal{P}_{q_2}^{q_1} v - v \|_{q_2} \leq c_1 \| \text{Log}_{q_1} p_1 \|_{q_2} = c_1 d_{\mathcal{M}}(p_1, q_1), \end{aligned}$$

which further imply that

$$\begin{aligned} & \| \mathcal{P}_{p_2}^{q_2} \mathcal{P}_{p_1}^{p_2} \mathcal{P}_{q_1}^{p_1} \mathcal{P}_{q_2}^{q_1} v - v \|_{q_2} = \| (\mathcal{P}_{p_2}^{q_2} \mathcal{P}_{p_1}^{p_2} \mathcal{P}_{q_2}^{q_1}) (\mathcal{P}_{p_1}^{q_2} \mathcal{P}_{q_1}^{p_1} \mathcal{P}_{q_2}^{q_1}) v - v \|_{q_2} \\ & \leq \| (\mathcal{P}_{p_2}^{q_2} \mathcal{P}_{p_1}^{p_2} \mathcal{P}_{q_2}^{q_1}) (\mathcal{P}_{p_1}^{q_2} \mathcal{P}_{q_1}^{p_1} \mathcal{P}_{q_2}^{q_1}) v - (\mathcal{P}_{p_1}^{q_2} \mathcal{P}_{q_1}^{p_1} \mathcal{P}_{q_2}^{q_1}) v \|_{q_2} + \| (\mathcal{P}_{p_1}^{q_2} \mathcal{P}_{q_1}^{p_1} \mathcal{P}_{q_2}^{q_1}) v - v \|_{q_2} \\ & \leq c_1 (d_{\mathcal{M}}(p_2, q_2) + d_{\mathcal{M}}(p_1, q_1)). \end{aligned}$$

According to Theorem 3 in [Pennec \(2019\)](#), we have

$$\|\text{Log}_{q_2} y - \mathcal{P}_{p_2}^{q_2} \text{Log}_{p_2} y\|_{q_2} \leq c_2 \|\text{Log}_{q_2} p_2\|_{q_2} \leq c_2 d_{\mathcal{M}}(p_2, q_2)$$

for some constant $c_2 > 0$ depending only on \mathcal{G} . The proof is then completed by taking $c = c_1 + c_2$. \square

Proof of Proposition 4.2. The proposition follows directly from Claims [A.1](#) and [A.2](#), and the observation $\sup_{\tau:|\tau-t|<h} d_{\mathcal{M}}(\mu(\tau), \hat{\mu}(\tau)) \leq \sup_{\tau:|\tau-t|<h} d_{\mathcal{M}}(\tilde{\mu}(\tau), \mu(\tau)) + \sup_{\tau:|\tau-t|<h} d_{\mathcal{M}}(\hat{\mu}(\tau), \tilde{\mu}(\tau))$.

Claim A.1. *If the assumptions in Proposition 4.2 hold, then*

$$\sup_{t \in \mathcal{T}} d_{\mathcal{M}}(\mu(t), \tilde{\mu}(t)) = O(h_{\mu}^2).$$

To establish the above claim, we first show that

$$\lim_{n \rightarrow \infty} \sup_{t \in \mathcal{T}} d_{\mathcal{M}}(\tilde{\mu}(t), \mu(t)) = 0. \quad (13)$$

To this end, we observe that

$$\begin{aligned} u_k(t) &= \mathbf{E}\{K_{h_{\mu}}(T-t) \times (T-t)^k\} = \int K_{h_{\mu}}(s-t) \times (s-t)^k f(s) ds \\ &= \int K(u) \times u^k h_{\mu}^k \times f(t+uh_{\mu}) du \\ &= h_{\mu}^k f(t) K_{1k} + h_{\mu}^{k+1} f'(t) K_{1,k+1} + O(h_{\mu}^{k+2}), \end{aligned} \quad (14)$$

$$\tau_{y,k}(t) := \mathbf{E}\{K_{h_{\mu}}(T-t) \times (T-t)^k \mid Y=y\} = h_{\mu}^k g_y(t) K_{1k} + h_{\mu}^{k+1} g'_y(t) K_{1,k+1} + O(h_{\mu}^{k+2}), \quad (15)$$

where $K_{a,k} := \int K^a(u) \times u^k du$ and the $O(h_{\mu}^{k+2})$ terms are uniform in $t \in \mathcal{T}$. Simple computation and Assumption [4.1](#) suggest that there exists a constant $c_1 > 0$ such that for large n ,

$$\sup_{t \in \mathcal{T}, y \in \mathcal{K}} \left| \frac{u_2(t)\tau_{y,0}(t) - u_1(t)\tau_{y,1}(t)}{\sigma_0^2(t)} - \frac{g_y(t)}{f(t)} \right| < c_1 h_{\mu}^2. \quad (16)$$

In addition, if $\mathcal{F}_{T,Y}$ denotes the joint distribution of (T, Y) , \mathcal{F}_Y is the distribution of Y , and $\mathcal{F}_{Y|T}, \mathcal{F}_{T|Y}$ are conditional distributions, then $d\mathcal{F}_{Y|T}(t, z)/d\mathcal{F}_Y(z) = g_z(t)/f(t)$, as shown in the proof of Theorem 3 of [Petersen and Müller \(2019\)](#). This implies that

$$\mathbf{E}\{d_{\mathcal{M}}^2(Y(t), y)\} = F(y, t) = \int d_{\mathcal{M}}^2(z, y) d\mathcal{F}_{Y|T}(t, z) = \int d_{\mathcal{M}}^2(z, y) \frac{g_z(t)}{f(t)} d\mathcal{F}_Y(z) = \mathbf{E}\left\{d_{\mathcal{M}}^2(Y, y) \frac{g_Y(t)}{f(t)}\right\}.$$

Based on the above, we deduce that

$$\begin{aligned} & \tilde{Q}_n(y, t) - \mathbf{E}\{d_{\mathcal{M}}^2(Y(t), y)\} \\ &= \mathbf{E}\{w(T, t, h_{\mu}) d_{\mathcal{M}}^2(Y, y)\} - \mathbf{E}\left\{d_{\mathcal{M}}^2(Y, y) \frac{g_Y(t)}{f(t)}\right\} \\ &= \mathbf{E}\{\mathbf{E}\{w(T, t, h_{\mu}) d_{\mathcal{M}}^2(Y, y) \mid Y\}\} - \mathbf{E}\left\{d_{\mathcal{M}}^2(Y, y) \frac{g_Y(t)}{f(t)}\right\} \\ &= \mathbf{E}\left\{d_{\mathcal{M}}^2(Y, y) \int_{\mathcal{T}} g_Y(s) \frac{1}{\sigma_0^2(t)} K_{h_{\mu}}(s-t) \times [u_2(t) - u_1(t)(s-t)] ds\right\} - \mathbf{E}\left\{d_{\mathcal{M}}^2(Y, y) \frac{g_Y(t)}{f(t)}\right\} \\ &= \mathbf{E}\left[d_{\mathcal{M}}^2(Y, y) \left\{ \frac{u_2(t)\tau_{Y,0}(t) - u_1(t)\tau_{Y,1}(t)}{\sigma_0^2(t)} - \frac{g_Y(t)}{f(t)} \right\}\right], \end{aligned} \quad (17)$$

where the last equality is partially due to the definition in (15). With (16), we further have

$$\sup_{t \in \mathcal{T}, y \in \mathcal{K}} |\tilde{Q}_n(y, t) - \mathbf{E}\{d_{\mathcal{M}}^2(Y(t), y)\}| \leq c_1 \text{diam}(\mathcal{K})^2 h_\mu^2. \quad (18)$$

According to Assumption 4.2(b), for any $\delta_0 > 0$,

$$\liminf_{n \rightarrow \infty} \inf_{d_{\mathcal{M}}(y, \tilde{\mu}(t)) > \delta_0, t \in \mathcal{T}} \{\tilde{Q}_n(y, t) - \tilde{Q}_n(\tilde{\mu}(t), t)\} > 0.$$

Then there exist $\epsilon > 0$ and $n_0 \geq 1$ such that for any $n > n_0$,

$$\inf_{d_{\mathcal{M}}(y, \tilde{\mu}(t)) > \delta_0, t \in \mathcal{T}} \{\tilde{Q}_n(y, t) - \tilde{Q}_n(\tilde{\mu}(t), t)\} > \epsilon \quad \text{and} \quad \sup_{t \in \mathcal{T}, y \in \mathcal{K}} |\tilde{Q}_n(y, t) - \mathbf{E}\{d_{\mathcal{M}}^2(Y(t), y)\}| < \frac{\epsilon}{3}.$$

These imply that

$$\inf_{d_{\mathcal{M}}(y, \tilde{\mu}(t)) > \delta_0} \mathbf{E}\{d_{\mathcal{M}}^2(Y(t), y)\} \geq \inf_{d_{\mathcal{M}}(y, \tilde{\mu}(t)) > \delta_0} \tilde{Q}_n(y, t) - \frac{\epsilon}{3} > \tilde{Q}_n(\tilde{\mu}(t), t) + \frac{2}{3}\epsilon > \mathbf{E}\{d_{\mathcal{M}}^2(Y(t), \tilde{\mu}(t))\} + \frac{\epsilon}{3}.$$

This further implies that the Fréchet mean of $Y(t)$, which is the minimizer of $F^*(y, t) = \mathbf{E}\{d_{\mathcal{M}}^2(Y(t), y)\}$ as a function of y , is within distance δ_0 of $\tilde{\mu}(t)$. Since $X(t)$ and $Y(y)$ share the same Fréchet mean $\mu(t)$, we conclude that $d_{\mathcal{M}}(\tilde{\mu}(t), \mu(t)) < \delta_0$ for all $t \in \mathcal{T}$, and thus (13) follows.

Now, according to Assumption 4.2(d) and (13), we deduce that

$$\tilde{Q}_n(\mu(t), t) - \tilde{Q}_n(\tilde{\mu}(t), t) > C_2 d_{\mathcal{M}}(\mu(t), \tilde{\mu}(t))^2.$$

On one hand, since $\mu(t)$ is the minimizer of $\mathbf{E}\{d_{\mathcal{M}}^2(Y(t), y)\}$, we have $\mathbf{E}\{d_{\mathcal{M}}^2(Y(t), \tilde{\mu}(t))\} - \mathbf{E}\{d_{\mathcal{M}}^2(Y(t), \mu(t))\} \geq 0$. Thus,

$$[\tilde{Q}_n(\mu(t), t) - \mathbf{E}\{d_{\mathcal{M}}^2(Y(t), \mu(t))\}] - [\tilde{Q}_n(\tilde{\mu}(t), t) - \mathbf{E}\{d_{\mathcal{M}}^2(Y(t), \tilde{\mu}(t))\}] > C_2 d_{\mathcal{M}}(\mu(t), \tilde{\mu}(t))^2.$$

On the other hand, by (17),

$$\begin{aligned} & [\tilde{Q}_n(\mu(t), t) - \mathbf{E}\{d_{\mathcal{M}}^2(Y(t), \mu(t))\}] - [\tilde{Q}_n(\tilde{\mu}(t), t) - \mathbf{E}\{d_{\mathcal{M}}^2(Y(t), \tilde{\mu}(t))\}] \\ & \leq \mathbf{E}\left[\{d_{\mathcal{M}}^2(Y, \mu(t)) - d_{\mathcal{M}}^2(Y, \tilde{\mu}(t))\} \times \left\{\frac{u_2(t)\tau_{Y,0}(t) - u_1(t)\tau_{Y,1}(t)}{\sigma_0^2(t)} - \frac{g_Y(t)}{f(t)}\right\}\right] \\ & \leq 2c_1 h_\mu^2 d_{\mathcal{M}}(\mu(t), \tilde{\mu}(t)) \times \text{diam}(\mathcal{K}). \end{aligned}$$

Therefore, $\sup_{t \in \mathcal{T}} d_{\mathcal{M}}(\mu(t), \tilde{\mu}(t)) \leq C_2^{-1} 2c_1 \text{diam}(\mathcal{K}) h_\mu^2 = O(h_\mu^2)$, as needed.

Claim A.2. *If the assumptions in Proposition 4.2 hold, then for any fixed t ,*

$$\sup_{\tau: |\tau - t| < h} d_{\mathcal{M}}(\hat{\mu}(t), \tilde{\mu}(t)) = O_p(h_\mu^{-\frac{1}{2}} m^{-\frac{1}{2}} n^{-\frac{1}{2}} + n^{-\frac{1}{2}}).$$

The proof of this claim is adapted from the proof of Theorem 4 of Petersen and Müller (2019), with extra care for the supremum $\sup_{\tau: |\tau - t| < h}$. We divide the proof of the claim into two steps. In the first step, we show that

$$\sup_{\tau \in B(t; h)} d_{\mathcal{M}}(\hat{\mu}(\tau), \tilde{\mu}(\tau)) = o_p(1), \quad (19)$$

where $B(t; h) = \{\tau : |\tau - t| < h\}$. In the second step, we derive the precise convergence rate.

Step 1: Recall that $\hat{w}(T_{ij}, t, h_\mu) = \frac{1}{\hat{\sigma}_0^2} K_{h_\mu}(T_{ij} - t) \times [\hat{u}_2(t) - \hat{u}_1(t)(T_{ij} - t)]$ and $w(T, t, h_\mu) = \frac{1}{\sigma_0^2} K_{h_\mu}(T - t) \times [u_2(t) - u_1(t)(T - t)]$. Then

$$\begin{aligned} \hat{Q}_n(y, t) - \tilde{Q}_n(y, t) &= \sum_i \lambda_i \sum_j \hat{w}(T_{ij}, t, h_\mu) d_{\mathcal{M}}^2(Y_{ij}, y) - \mathbf{E}\{w(T, t, h_\mu) d_{\mathcal{M}}^2(Y, y)\} \\ &= \sum_i \lambda_i \sum_j \{\hat{w}(T_{ij}, t, h_\mu) d_{\mathcal{M}}^2(Y_{ij}, y) - w(T_{ij}, t, h_\mu) d_{\mathcal{M}}^2(Y_{ij}, y)\} \\ &\quad + \sum_i \lambda_i \sum_j \{w(T_{ij}, t, h_\mu) d_{\mathcal{M}}^2(Y_{ij}, y) - \mathbf{E}\{w(T, t, h_\mu) d_{\mathcal{M}}^2(Y, y)\}\}. \end{aligned} \quad (20)$$

To deal with the first term of (20), we observe that

$$\left| \hat{w}(T_{ij}, t, h_\mu) - w(T, t, h_\mu) \right| \leq \left| \frac{\hat{u}_2(t)}{\hat{\sigma}_0^2(t)} - \frac{u_2(t)}{\sigma_0^2(t)} \right| K_{h_\mu}(T_{ij} - t) + \left| \frac{\hat{u}_1(t)}{\hat{\sigma}_0^2(t)} - \frac{u_1(t)}{\sigma_0^2(t)} \right| (T_{ij} - t) K_{h_\mu}(T_{ij} - t). \quad (21)$$

From (14) and the symmetry of the kernel function K , we have

$$\begin{aligned} \sup_{\tau \in B(t; h)} u_0(\tau) &= \sup_{\tau \in B(t; h)} f(\tau) + O(h_\mu^2), \\ \sup_{\tau \in B(t; h)} u_1(\tau) &= \sup_{\tau \in B(t; h)} f'(\tau) K_{1,2} h_\mu^2 + O(h_\mu^3), \\ \sup_{\tau \in B(t; h)} u_2(\tau) &= \sup_{\tau \in B(t; h)} f(\tau) K_{2,2} h_\mu^2 + O(h_\mu^4). \end{aligned}$$

The estimator $\hat{u}_k(t)$ is unbiased for $u_k(t)$ and

$$\begin{aligned} \mathbf{E} \sup_{\tau \in B(t; h)} \left| \hat{u}_k(\tau) - u_k(\tau) \right|^2 &\leq \sum_i \sum_j \lambda_i^2 \mathbf{E} \sup_{\tau \in B(t; h)} K_{h_\mu}^2(T_{ij} - \tau) \times (T_{ij} - \tau)^{2k} \\ &= \frac{1}{mn} \int \sup_{\tau \in B(t; h)} K_{h_\mu}^2(s - \tau) \times (s - \tau)^{2k} f(s) ds \\ &= O\left(\frac{h_\mu^{2k-1}}{mn}\right). \end{aligned}$$

With these, simple computation leads to

$$\sup_{\tau \in B(t; h)} \left| \frac{\hat{u}_2(\tau)}{\hat{\sigma}_0^2(\tau)} - \frac{u_2(\tau)}{\sigma_0^2(\tau)} \right| = O_p(h_\mu^{-\frac{1}{2}} m^{-\frac{1}{2}} n^{-\frac{1}{2}}) \quad \text{and} \quad \sup_{\tau \in B(t; h)} \left| \frac{\hat{u}_1(\tau)}{\hat{\sigma}_0^2(\tau)} - \frac{u_1(\tau)}{\sigma_0^2(\tau)} \right| = O_p(h_\mu^{-\frac{3}{2}} m^{-\frac{1}{2}} n^{-\frac{1}{2}}). \quad (22)$$

Besides,

$$\begin{aligned} \mathbf{E} \sup_{\tau \in B(t; h)} K_{h_\mu}(T_{ij} - \tau) &= O\left(\frac{h}{h_\mu} + 1\right) = O(1), \\ \mathbf{E} \sup_{\tau \in B(t; h)} K_{h_\mu}(T_{ij} - \tau) \times (T_{ij} - \tau) &= O\left(\left(\frac{h}{h_\mu} + 1\right) h_\mu\right) = O(h_\mu). \end{aligned}$$

Combining them with (21) and (22), we conclude that the first term of (20) has the rate

$$\sup_{\tau \in B(t; h), y \in \mathcal{K}} \sum_i \lambda_i \sum_j \{\hat{w}(T_{ij}, \tau, h_\mu) - w(T_{ij}, \tau, h_\mu)\} d_{\mathcal{M}}^2(Y_{ij}, y) = O_p(h_\mu^{-\frac{1}{2}} m^{-\frac{1}{2}} n^{-\frac{1}{2}}).$$

For the second term of (20), define

$$g(y, \tau) = \frac{1}{m} \sum_{j=1}^m w(T_{1j}, \tau, h_\mu) d_{\mathcal{M}}^2(Y_{1j}, y),$$

which is Lipschitz continuous in (y, τ) , and consider the class of random variables $\{g(y, \tau) : y \in \mathcal{K}, \tau \in B(t; h)\}$. The elements in the class are viewed as measurable functions mapping the sample space Ω into \mathbb{R} . The class has an envelope function given by

$$H = \frac{\text{diam}(\mathcal{K})^2}{m} \sum_{j=1}^m \sup_{\tau \in B(t; h)} |w(T_{1j}, \tau, h_\mu)|.$$

From the analysis in Step 1 one can show that $\mathbf{E}\{H^2\} = O(\frac{1}{mh} + 1)$. Now, according to Theorems 2.7.11 and 2.14.2 in van der Vaart and Wellner (1996)

$$\mathbf{E} \left| \sup_{\substack{y \in \mathcal{K} \\ \tau \in B(t; h)}} \sum_i \lambda_i \sum_j [w(T_{ij}, \tau, h_\mu) d_{\mathcal{M}}^2(Y_{ij}, y) - \mathbf{E}\{w(T, \tau, h_\mu) d_{\mathcal{M}}^2(Y, y)\}] \right| = O(n^{-\frac{1}{2}} m^{-\frac{1}{2}} h_\mu^{-\frac{1}{2}} + n^{-\frac{1}{2}}).$$

Combining this with the result for the first term, we deduce that,

$$\sup_{y \in \mathcal{K}} \sup_{\tau \in B(t; h)} |\hat{Q}_n(y, \tau) - \tilde{Q}_n(y, \tau)| = O_p(h_\mu^{-\frac{1}{2}} m^{-\frac{1}{2}} n^{-\frac{1}{2}} + n^{-\frac{1}{2}}) = o_p(1).$$

Now (19) follows from the argument in the proof of Lemma 2 in Petersen and Müller (2019), if we verify that for any $\kappa > 0$,

$$\lim_{\delta \rightarrow 0} \limsup_{n \rightarrow \infty} \Pr \left\{ \sup_{d_{\mathcal{M}}(y_1, y_2) < \delta, \tau \in B(t; h)} |\{\hat{Q}_n(y_1, \tau) - \tilde{Q}_n(y_1, \tau)\} - \{\hat{Q}_n(y_2, \tau) - \tilde{Q}_n(y_2, \tau)\}| > \kappa \right\} = 0.$$

One can show that $\sup_{\tau \in B(t; h)} |\hat{\omega}(T_{ij}, \tau, h_\mu)| = O_p(1)$ and $\mathbf{E} \sup_{\tau \in B(t; h)} |\omega(T, \tau, h_\mu)| = O(1)$, which further imply that $\sup_{\tau \in B(t; h)} |\hat{Q}_n(y_1, \tau) - \hat{Q}_n(y_2, \tau)| = O_p(d_{\mathcal{M}}(y_1, y_2))$ and $\sup_{\tau \in B(t; h)} |\tilde{Q}_n(y_1, \tau) - \tilde{Q}_n(y_2, \tau)| = O(d_{\mathcal{M}}(y_1, y_2))$, and thus the above equation is verified.

Step 2: Define $D(Y_{ij}, y, t) := d_{\mathcal{M}}^2(Y_{ij}, y) - d_{\mathcal{M}}^2(Y_{ij}, \tilde{\mu}(t))$ and $S_n(y, t) = \hat{Q}_n(y, t) - \tilde{Q}_n(y, t)$, then

$$\begin{aligned} & |S_n(y, t) - S_n(\tilde{\mu}(t), t)| \\ &= \left| \sum_i \lambda_i \sum_j \hat{w}(T_{ij}, t, h_\mu) [d_{\mathcal{M}}^2(Y_{ij}, y) - d_{\mathcal{M}}^2(Y_{ij}, \tilde{\mu}(t))] - \mathbf{E}\{w(T, t, h_\mu) [d_{\mathcal{M}}^2(Y_{ij}, y) - d_{\mathcal{M}}^2(Y_{ij}, \tilde{\mu}(t))]\} \right| \\ &= \left| \sum_i \lambda_i \sum_j \hat{w}(T_{ij}, t, h_\mu) D(Y_{ij}, y, t) - \mathbf{E}\{w(T, t, h_\mu) D(Y, y, t)\} \right| \\ &\leq \sum_i \lambda_i \sum_j |\hat{w}(T_{ij}, t, h_\mu) - w(T_{ij}, t, h_\mu)| \times |D(Y_{ij}, y, t)| \end{aligned} \quad (23)$$

$$+ \sum_i \lambda_i \sum_j |w(T_{ij}, t, h_\mu) D(Y_{ij}, y, t) - \mathbf{E}\{w(T_{ij}, t, h_\mu) D(Y_{ij}, y, t)\}|. \quad (24)$$

Since $\sup_{\{d_{\mathcal{M}}(y, \tilde{\mu}(\tau)) < \delta, \tau \in B(t; h)\}} |D(Y_{ij}, y, \tau)| \leq 3\delta \times \text{diam}(\mathcal{K})$, (23) can be bounded by

$$\sup_{\substack{d_{\mathcal{M}}(y, \tilde{\mu}(\tau)) < \delta \\ \tau \in B(t; h)}} \sum_i \lambda_i \sum_j |\hat{w}(T_{ij}, \tau, h_\mu) - w(T_{ij}, \tau, h_\mu)| \times |D(Y_{ij}, y, \tau)| = O_p(\delta h_\mu^{-\frac{1}{2}} m^{-\frac{1}{2}} n^{-\frac{1}{2}}).$$

Thus, for $R < 0$, if we define the event

$$B_R := \left\{ \sup_{\substack{d_{\mathcal{M}}(y, \tilde{\mu}(\tau)) < \delta \\ \tau \in B(t; h)}} \sum_i \lambda_i \sum_j |\hat{w}(T_{ij}, \tau, h_\mu) - w(T_{ij}, \tau, h_\mu)| \times |D(Y_{ij}, y, \tau)| < R \delta h_\mu^{-\frac{1}{2}} m^{-\frac{1}{2}} n^{-\frac{1}{2}} \right\},$$

then B_R satisfies

$$\lim_{R \rightarrow \infty} \limsup_{n \rightarrow \infty} \Pr\{B_R\} = 1.$$

To bound (24), we again utilize Theorems 2.7.11 and 2.14.2 in [van der Vaart and Wellner \(1996\)](#). Define

$$g(y, \tau) = \frac{1}{m} \sum_{j=1}^m w(T_{1j}, \tau, h_\mu) d_{\mathcal{M}}(Y_{1j}, y),$$

which is Lipschitz continuous in (y, τ) , and consider the class of random variables

$$\{g(y, \tau) - g(\tilde{\mu}(\tau), \tau) : d_{\mathcal{M}}(y, \tilde{\mu}(\tau)) < \delta \text{ and } \tau \in B(t; h)\}.$$

The elements in the class are viewed as measurable functions mapping the sample space Ω into \mathbb{R} . The class has an envelope function given by

$$H = \frac{\delta}{m} \sum_{j=1}^m \sup_{\tau \in B(t; h)} |w(T_{ij}, \tau, h_\mu)|.$$

One can show that $\mathbf{E}\{H^2\} = O(\delta^2(\frac{1}{mh} + 1))$. By the aforementioned theorems in [van der Vaart and Wellner \(1996\)](#), for sufficiently small $\delta > 0$,

$$\mathbf{E} \left| \sup_{\substack{d_{\mathcal{M}}(y, \tilde{\mu}(\tau)) < \delta \\ \tau \in B(t; h)}} \sum_i \lambda_i \sum_j [w(T_{ij}, \tau, h_\mu) D(Y_{ij}, y, \tau) - \mathbf{E}\{w(T_{ij}, \tau, h_\mu) D(Y_{ij}, y, \tau)\}] \right| = O(\delta n^{-\frac{1}{2}} m^{-\frac{1}{2}} h_\mu^{-\frac{1}{2}} + \delta n^{-\frac{1}{2}}).$$

Thus, there exists a constant $c_1 > 0$ such that

$$\mathbf{E} \left\{ I_{B_R} \sup_{\substack{d_{\mathcal{M}}(y, \tilde{\mu}(\tau)) < \delta \\ \tau \in B(t; h)}} |S_n(y, \tau) - S_n(\tilde{\mu}(t), \tau)| \right\} \leq (c_1 + R)(\delta n^{-\frac{1}{2}} m^{-\frac{1}{2}} h_\mu^{-\frac{1}{2}} + \delta n^{-\frac{1}{2}}).$$

According to Assumption 4.2(d), for sufficiently large n so that $d_{\mathcal{M}}(\hat{\mu}(t), \tilde{\mu}(t)) < \eta_2$ for all $t \in \mathcal{T}$, we have

$$\tilde{Q}_n(\hat{\mu}(t), t) - \tilde{Q}_n(\tilde{\mu}(t), t) \geq C_2 d_{\mathcal{M}}(\hat{\mu}(t), \tilde{\mu}(t))^2.$$

Since $\hat{\mu}(t)$ is the minimizer of $\hat{Q}_n(y, t)$, $\hat{Q}_n(\tilde{\mu}(t), t) - \hat{Q}_n(\hat{\mu}(t), t) \geq 0$. Thus for sufficiently large n so that $d_{\mathcal{M}}(\hat{\mu}(t), \tilde{\mu}(t)) < \eta_2$ for all $t \in \mathcal{T}$, we have the following inequality

$$S_n(\tilde{\mu}(t), t) - S_n(\hat{\mu}(t), t) \geq C_2 d_{\mathcal{M}}(\hat{\mu}(t), \tilde{\mu}(t))^2.$$

For any $M > 0$, define $a_n = n^{-\frac{1}{2}} m^{-\frac{1}{2}} h_\mu^{-\frac{1}{2}} + n^{-\frac{1}{2}}$, $B_j := \{y : 2^j M a_n \leq \sup_{\tau \in B(t; h)} d_{\mathcal{M}}(\hat{\mu}(\tau), \tilde{\mu}(\tau)) \leq 2^{j+1} M a_n\}$

and $B_C := \{\sup_{\tau \in B(t;h)} d_{\mathcal{M}}(\hat{\mu}(\tau), \tilde{\mu}(\tau)) > \frac{1}{2}\eta_1\}$. Then for any $R > 0$ and j_0 satisfying $\frac{1}{2}\eta_1 < 2^{j_0+1}Ma_n \leq \eta_1$,

$$\begin{aligned}
& \Pr\left\{\sup_{\tau \in B(t;h)} d_{\mathcal{M}}(\hat{\mu}(\tau), \tilde{\mu}(\tau)) > Ma_n\right\} \\
& \leq \sum_{j=0}^{j_0} \Pr(B_j \cap B_R) + \Pr(B_C \cap B_R) + \Pr(\Omega \setminus B_R) \\
& \leq \sum_{j=0}^{j_0} \Pr\left(B_j \cap \left\{\sup_{\tau \in B(t;h)} |S_n(\tilde{\mu}(\tau), \tau) - S_n(\hat{\mu}(\tau), \tau)| > C_2(2^j Ma_n)^2\right\} \cap B_R\right) + \Pr\{B_C\} + \Pr(\Omega \setminus B_R) \\
& \leq \sum_{j=0}^{j_0} \Pr\left(I_{B_R} \sup_{d_{\mathcal{M}}(y, \tilde{\mu}(\tau)) \leq 2^{j+1}Ma_n, \tau \in B(t;h)} |S_n(\tilde{\mu}(\tau), \tau) - S_n(y, \tau)| > C_2(2^j Ma_n)^2\right) + \Pr\{B_C\} + \Pr(\Omega \setminus B_R) \\
& \leq (C_3 + R) \sum_{j=0}^{j_0} \frac{2^{j+1}Ma_n^2}{C_2(2^j Ma_n)^2} + \Pr\{B_C\} + \Pr(\Omega \setminus B_R) \\
& \leq \frac{4(C_3+R)}{C_2M} + \Pr\{B_C\} + \Pr(\Omega \setminus B_R).
\end{aligned}$$

According to (19), $\lim_{n \rightarrow \infty} \Pr\{B_C\} = 0$. Together with $\lim_{R \rightarrow \infty} \limsup_{n \rightarrow \infty} \Pr\{B_R\} = 1$, it implies that for any $\epsilon > 0$, there exist n_0 and R_0 such that for any $n > n_0$,

$$\Pr\{\Omega \setminus B_{R_0}\} < \frac{\epsilon}{3} \quad \text{and} \quad \Pr\{B_C\} < \frac{\epsilon}{3}.$$

For $M > \frac{12(C_3+R_0)}{\epsilon C_2}$, we have

$$\Pr\left\{\sup_{\tau \in B(t;h)} d_{\mathcal{M}}(\hat{\mu}(\tau), \tilde{\mu}(\tau)) > Ma_n\right\} \leq \frac{4(C_3+R_0)}{C_2M} + \Pr\{B_C\} + \Pr(\Omega \setminus B_{R_0}) \leq \epsilon.$$

Therefore,

$$\lim_{M \rightarrow \infty} \limsup_{n \rightarrow \infty} \Pr\left\{\sup_{\tau \in B(t;h)} d_{\mathcal{M}}(\hat{\mu}(\tau), \tilde{\mu}(\tau)) > Ma_n\right\} = 0.$$

This yields the desired convergence rate of Claim A.2 and completes the proof of Proposition 4.2. \square

Proof of Theorem 4.1. We divide the proof into three steps. In the first step, we show that the convergence rate depends on some terms of the numerator of (27). In the second step and third step, we address them separately.

Step 1. Define $\gamma := \hat{\mu}$ to simplify notation in the sequel. Since the parallel transport $\mathcal{P}_{(\gamma(s), \gamma(t))}^{(\mu(s), \mu(t))}$ preserves the fiber metric according to Theorem 2.4,

$$\begin{aligned}
\mathcal{P}_{(\gamma(s), \gamma(t))}^{(\mu(s), \mu(t))} \hat{\mathcal{C}}(s, t) &= \arg_{\beta_0, \beta_1, \beta_2 \in \mathbb{L}(\mu(s), \mu(t))} \min \left\{ \sum_i \nu_i \sum_{j \neq k} \left\| \mathcal{P}_{(\gamma(s), \gamma(t))}^{(\mu(s), \mu(t))} \mathcal{P}_{(\gamma(T_{ij}), \gamma(T_{ik}))}^{(\mu(s), \mu(t))} \hat{\mathcal{C}}_{i,jk} \right. \right. \\
&\quad \left. \left. - \beta_0 - \beta_1(T_{ij} - s) - \beta_2(T_{ik} - t) \right\|_{G(\mu(s), \mu(t))}^2 K_{h_C}(s - T_{ij}) K_{h_C}(t - T_{ik}) \right\}.
\end{aligned}$$

Simple computation shows that

$$\mathcal{P}_{(\gamma(s), \gamma(t))}^{(\mu(s), \mu(t))} \hat{\mathcal{C}}(s, t) - \mathcal{C}(s, t) = \frac{(S_{20}S_{02} - S_{11}^2)R_{00} - (S_{10}S_{02} - S_{01}S_{11})R_{10} + (S_{10}S_{11} - S_{01}S_{20})R_{01}}{(S_{20}S_{02} - S_{11}^2)S_{00} - (S_{10}S_{02} - S_{01}S_{11})S_{10} + (S_{10}S_{11} - S_{01}S_{20})S_{01}}, \quad (25)$$

where R_{ab} and S_{ab} are defined as

$$R_{ab} := \sum_i \nu_i \sum_{j \neq k} \varpi(T_{ij}, T_{ik}) \left(\frac{T_{ij}-s}{h_C} \right)^a \left(\frac{T_{ik}-t}{h_C} \right)^b \left\{ \mathcal{P}_{(\gamma(s), \gamma(t))}^{(\mu(s), \mu(t))} \mathcal{P}_{(\gamma(T_{ij}), \gamma(T_{ik}))}^{(\gamma(s), \gamma(t))} \hat{\mathcal{C}}_{i,jk} - \mathcal{C}(s, t) \right\},$$

$$S_{ab} := \sum_i \nu_i \sum_{j \neq k} \varpi(T_{ij}, T_{ik}) \left(\frac{T_{ij}-s}{h_C} \right)^a \left(\frac{T_{ik}-t}{h_C} \right)^b,$$

with $\varpi(s', t') = K_{h_C}(s - s')K_{h_C}(t - t')$ for $s', t' \in \mathcal{T}$.

Define $\tilde{\mathcal{C}}_{i,jk} := \mathcal{P}_{(\mu(T_{ij}), \mu(T_{ik}))}^{(\mu(s), \mu(t))} (\text{Log}_{\mu(T_{ij})} Y_{ij} \otimes \text{Log}_{\mu(T_{ik})} Y_{ik}) \in \mathbb{L}(\mu(s), \mu(t))$. We consider the decomposition

$$\mathcal{P}_{(\gamma(s), \gamma(t))}^{(\mu(s), \mu(t))} \mathcal{P}_{(\gamma(T_{ij}), \gamma(T_{ik}))}^{(\gamma(s), \gamma(t))} \hat{\mathcal{C}}_{i,jk} - \mathcal{C}(s, t) = \left\{ \mathcal{P}_{(\gamma(s), \gamma(t))}^{(\mu(s), \mu(t))} \mathcal{P}_{(\gamma(T_{ij}), \gamma(T_{ik}))}^{(\gamma(s), \gamma(t))} \hat{\mathcal{C}}_{i,jk} - \tilde{\mathcal{C}}_{i,jk} \right\} + \left\{ \tilde{\mathcal{C}}_{i,jk} - \mathcal{C}(s, t) \right\} \quad (26)$$

and split R_{ab} into $R_{ab} = R_{ab,1} + R_{ab,2}$ accordingly, where

$$R_{ab,1} := \sum_i \nu_i \sum_{j \neq k} \varpi(T_{ij}, T_{ik}) \left(\frac{T_{ij}-s}{h_C} \right)^a \left(\frac{T_{ik}-t}{h_C} \right)^b \left\{ \mathcal{P}_{(\gamma(s), \gamma(t))}^{(\mu(s), \mu(t))} \mathcal{P}_{(\gamma(T_{ij}), \gamma(T_{ik}))}^{(\gamma(s), \gamma(t))} \hat{\mathcal{C}}_{i,jk} - \tilde{\mathcal{C}}_{i,jk} \right\},$$

$$R_{ab,2} := \sum_i \nu_i \sum_{j \neq k} \varpi(T_{ij}, T_{ik}) \left(\frac{T_{ij}-s}{h_C} \right)^a \left(\frac{T_{ik}-t}{h_C} \right)^b \left\{ \tilde{\mathcal{C}}_{i,jk} - \mathcal{C}(s, t) \right\}.$$

Combining (25) and (26), we can see that

$$\begin{aligned} \mathcal{P}_{(\gamma(s), \gamma(t))}^{(\mu(s), \mu(t))} \hat{\mathcal{C}}(s, t) - \mathcal{C}(s, t) &= \frac{(S_{20}S_{02} - S_{11}^2)[R_{00,1} + R_{00,2} - \partial_s \mathcal{C}(s, t)h_C S_{10} - \partial_t \mathcal{C}(s, t)h_C S_{01}]}{(S_{20}S_{02} - S_{11}^2)S_{00} - (S_{10}S_{02} - S_{01}S_{11})S_{10} + (S_{10}S_{11} - S_{01}S_{20})S_{01}} \\ &\quad - \frac{(S_{10}S_{02} - S_{01}S_{11})[R_{10,1} + R_{10,2} - \partial_s \mathcal{C}(s, t)h_C S_{20} - \partial_t \mathcal{C}(s, t)h_C S_{11}]}{(S_{20}S_{02} - S_{11}^2)S_{00} - (S_{10}S_{02} - S_{01}S_{11})S_{10} + (S_{10}S_{11} - S_{01}S_{20})S_{01}} \\ &\quad + \frac{(S_{10}S_{11} - S_{01}S_{20})[R_{01,1} + R_{01,2} - \partial_s \mathcal{C}(s, t)h_C S_{11} - \partial_t \mathcal{C}(s, t)h_C S_{02}]}{(S_{20}S_{02} - S_{11}^2)S_{00} - (S_{10}S_{02} - S_{01}S_{11})S_{10} + (S_{10}S_{11} - S_{01}S_{20})S_{01}}. \end{aligned} \quad (27)$$

According to Lemma 4 in Zhang and Wang (2016),

$$\sup_{s, t \in \mathcal{T}} |S_{ab} - \mathbf{E}S_{ab}| = o_p(1) \quad \text{and} \quad \sup_{s, t \in \mathcal{T}} \mathbf{E}S_{ab} \asymp 1. \quad (28)$$

Therefore, the convergence rate of (25) depends on $R_{ab,1}$ and $R_{ab,2} - \partial_s \mathcal{C}(s, t)h_C S_{a+1,b} - \partial_t \mathcal{C}(s, t)h_C S_{a,b+1}$.

Step 2. In this step, we will derive the rate of $R_{ab,1}$ in Equation (27). According to the definition of \mathcal{P} in (4), the first part in Equation (26) is $(\mathcal{P}_{\gamma(s)}^{\mu(s)} \mathcal{P}_{\gamma(T_{ij})}^{\gamma(s)} \text{Log}_{\gamma(T_{ij})} Y_{ij}) \otimes (\mathcal{P}_{\gamma(t)}^{\mu(t)} \mathcal{P}_{\gamma(T_{ik})}^{\gamma(t)} \text{Log}_{\gamma(T_{ik})} Y_{ik}) - (\mathcal{P}_{\mu(T_{ij})}^{\mu(s)} \text{Log}_{\mu(T_{ij})} Y_{ij}) \otimes (\mathcal{P}_{\mu(T_{ik})}^{\mu(t)} \text{Log}_{\mu(T_{ik})} Y_{ik})$. Then according to Assumption 4.1(b) and Lemma 4.1, its rate is

$$\left\| \mathcal{P}_{(\gamma(s), \gamma(t))}^{(\mu(s), \mu(t))} \mathcal{P}_{(\gamma(T_{ij}), \gamma(T_{ik}))}^{(\gamma(s), \gamma(t))} \hat{\mathcal{C}}_{i,jk} - \tilde{\mathcal{C}}_{i,jk} \right\|_G = O \left(\sup_{\tau: |\tau-s| < h_C \text{ or } |\tau-t| < h_C} d_{\mathcal{M}}(\gamma(\tau), \mu(\tau)) \right).$$

By Proposition 4.2, we conclude that

$$R_{ab,1} = O_P \left(h_\mu^2 + \sqrt{\frac{1}{n} + \frac{1}{nmh_\mu}} \right).$$

Step 3. In this step, we first analyze the term $R_{00,2} - \partial_s \mathcal{C}(s, t)h_C S_{10} - \partial_t \mathcal{C}(s, t)h_C S_{01}$ in (27), which equals to

$$U := \sum_i \nu_i \sum_{j \neq k} \varpi(T_{ij}, T_{ik}) \left\{ \tilde{\mathcal{C}}_{i,jk} - \mathcal{C}(s, t) - \partial_s \mathcal{C}(s, t)(T_{ij} - s) - \partial_t \mathcal{C}(s, t)(T_{ik} - t) \right\}.$$

We start with bounding its mean. Let $\mathbb{T} = \{T_{ij} : i = 1, \dots, n, j = 1, \dots, m_i\}$ and observe that

$$\mathbf{E}(\tilde{\mathcal{C}}_{i,jk} \mid \mathbb{T}) = \mathcal{P}_{(\mu(T_{ij}), \mu(T_{ik}))}^{(\mu(s), \mu(t))} \mathcal{C}(T_{ij}, T_{ik}).$$

In addition, since \mathcal{C} is twice differentiable and the parallel transport \mathcal{P} is depicted by a partial differential equation, we have the following Taylor expansion at (s, t) ,

$$\begin{aligned} & \mathcal{P}_{(\mu(T_{ij}), \mu(T_{ik}))}^{(\mu(s), \mu(t))} \mathcal{C}(T_{ij}, T_{ik}) \\ &= \mathcal{C}(s, t) + \partial_s \mathcal{C}(s, t)(T_{ij} - s) + \partial_t \mathcal{C}(s, t)(T_{ik} - t) + O(h_{\mathcal{C}}^2) \end{aligned} \quad (29)$$

for all T_{ij}, T_{ik} such that $|T_{ij} - s| < h_{\mathcal{C}}$ and $|T_{ik} - t| < h_{\mathcal{C}}$, where $O(h_{\mathcal{C}}^2)$ is uniform over all T_{ij} and T_{ik} due to Assumption 4.3 and the compactness of \mathcal{K} . Then we further deduce that

$$\begin{aligned} \mathbf{E}(U) &= \mathbf{E} \left\{ \mathbf{E} \left[\sum_i \nu_i \sum_{j \neq k} \varpi(T_{ij}, T_{ik}) \left\{ \tilde{\mathcal{C}}_{i,jk} - \mathcal{C}(s, t) - \partial_s \mathcal{C}(s, t)(T_{ij} - s) - \partial_t \mathcal{C}(s, t)(T_{ik} - t) \right\} \middle| \mathbb{T} \right] \right\} \\ &= \mathbf{E} \left[\sum_i \nu_i \sum_{j \neq k} \varpi(T_{ij}, T_{ik}) \left\{ \mathcal{P}_{(\mu(T_{ij}), \mu(T_{ik}))}^{(\mu(s), \mu(t))} \mathcal{C}(T_{ij}, T_{ik}) - \mathcal{C}(s, t) - \partial_s \mathcal{C}(s, t)(T_{ij} - s) - \partial_t \mathcal{C}(s, t)(T_{ik} - t) \right\} \right] \\ &= \mathbf{E} \left\{ \sum_i \nu_i \sum_{j \neq k} \varpi(T_{ij}, T_{ik}) \times O(h_{\mathcal{C}}^2) \right\} = O(h_{\mathcal{C}}^2). \end{aligned}$$

Next, the independence of trajectories implies that

$$\mathbf{E} \|U - \mathbf{E}U\|_G^2 = \sum_{i=1}^n \nu_i^2 \mathbf{E} \left\| \sum_{j \neq k} (U_{i,jk} - \mathbf{E}U_{i,jk}) \right\|_G^2 \leq \sum_{i=1}^n \nu_i^2 \mathbf{E} \left\| \sum_{j \neq k} U_{i,jk} \right\|_G^2, \quad (30)$$

where $U_{i,jk} = \varpi(T_{ij}, T_{ik}) \left\{ \tilde{\mathcal{C}}_{i,jk} - \mathcal{P}_{(\mu(T_{ij}), \mu(T_{ik}))}^{(\mu(s), \mu(t))} \mathcal{C}(T_{ij}, T_{ik}) \right\}$. To ease notation, we denote $\Delta_{i,jk} = \tilde{\mathcal{C}}_{i,jk} - \mathcal{P}_{(\mu(T_{ij}), \mu(T_{ik}))}^{(\mu(s), \mu(t))} \mathcal{C}(T_{ij}, T_{ik})$ and $H(s_1, s_2, t_1, t_2) = K_{h_{\mathcal{C}}}(s - s_1)K_{h_{\mathcal{C}}}(s - s_2)K_{h_{\mathcal{C}}}(t - t_1)K_{h_{\mathcal{C}}}(t - t_2)$. Then, we have

$$\begin{aligned} \left\| \sum_{j \neq k} U_{i,jk} \right\|_G^2 &= \sum_{j \neq k} H(T_{ij}, T_{ij}, T_{ik}, T_{ik}) \|\Delta_{i,jk}\|_G^2 \\ &\quad + \sum_j \sum_{k_1 \neq k_2} H(T_{ij}, T_{ij}, T_{ik_1}, T_{ik_2}) G_{(\mu(s), \mu(t))}(\Delta_{i,jk_1}, \Delta_{i,jk_2}) \\ &\quad + \sum_k \sum_{j_1 \neq j_2} H(T_{ij_1}, T_{ij_2}, T_{ik}, T_{ik}) G_{(\mu(s), \mu(t))}(\Delta_{i,j_1k}, \Delta_{i,j_2k}) \\ &\quad + \sum_{j_1 \neq j_2, k_1 \neq k_2} H(T_{ij_1}, T_{ij_2}, T_{ik_1}, T_{ik_2}) G_{(\mu(s), \mu(t))}(\Delta_{i,j_1k_1}, \Delta_{i,j_2k_2}) \\ &\leq c_{\mathcal{K}} \sum_{j \neq k} H(T_{ij}, T_{ij}, T_{ik}, T_{ik}) + c_{\mathcal{K}} \sum_j \sum_{k_1 \neq k_2} H(T_{ij}, T_{ij}, T_{ik_1}, T_{ik_2}) \\ &\quad + c_{\mathcal{K}} \sum_k \sum_{j_1 \neq j_2} H(T_{ij_1}, T_{ij_2}, T_{ik}, T_{ik}) + c_{\mathcal{K}} \sum_{j_1 \neq j_2, k_1 \neq k_2} H(T_{ij_1}, T_{ij_2}, T_{ik_1}, T_{ik_2}), \end{aligned}$$

where $c_{\mathcal{K}} > 0$ is an absolute constant depending only on \mathcal{K} . This implies that

$$\mathbf{E} \left\| \sum_{j \neq k} U_{i,jk} \right\|_G^2 \leq c_{\mathcal{K}} c_{K,f} (m^2 h_{\mathcal{C}}^{-2} + m^3 h_{\mathcal{C}}^{-1} + m^4) \leq c_{\mathcal{K}} c_{K,f} (m^2 h_{\mathcal{C}}^{-2} + m^4), \quad (31)$$

where $c_{K,f} > 0$ is an absolute constant depending only on K and the density function f of T . Combining (30), (31) and $v_i \equiv 1/(nm(m-1))$, we deduce that $\mathbf{E}\|U - \mathbf{E}U\|_G^2 = O(n^{-1} + n^{-1}m^{-1}h_C^{-1} + n^{-1}m^{-2}h_C^{-2})$. This result, together with $\mathbf{E}U = O(h_C^2)$ and Markov inequality, shows that $R_{00,2} - \partial_s \mathcal{C}(s, t)h_C S_{10} - \partial_t \mathcal{C}(s, t)h_C S_{01} = O_P(h_C^2 + n^{-1/2} + n^{-1/2}m^{-1}h_C^{-1})$.

Similar arguments can show that the terms $R_{10,2} - \partial_s \mathcal{C}(s, t)h_C S_{20} - \partial_t \mathcal{C}(s, t)h_C S_{11}$ and $R_{01,2} - \partial_s \mathcal{C}(s, t)h_C S_{11} - \partial_t \mathcal{C}(s, t)h_C S_{02}$ in (27) are of the same order. The equation (9) is then obtained by inserting the results in Steps 2 and 3 into Step 1. \square

Proof of Theorem 4.2. Similar to the proof of Theorem 4.1, we only need to consider the uniform rate of the term $R_{00,1} + R_{00,2} - \partial_s \mathcal{C}(s, t)h_C S_{10} - \partial_t \mathcal{C}(s, t)h_C S_{01}$ in (27).

Due to boundedness of \mathcal{K} and Lemma 4.1, we have

$$\sup_{s,t} \|\mathcal{P}_{(\gamma(s), \gamma(t))}^{(\mu(s), \mu(t))} \mathcal{P}_{(\gamma(T_{ij}), \gamma(T_{ik}))}^{(\gamma(s), \gamma(t))} \hat{\mathcal{C}}_{i,jk} - \tilde{\mathcal{C}}_{i,jk}\|_G \leq C \sup_{\tau} d_{\mathcal{M}}(\gamma(\tau), \mu(\tau)).$$

Therefore, according to (28) and Proposition 4.1 we deduce that

$$\sup_{s,t} \|R_{00,1}\|_G \leq c \left(\sup_{s,t} |S_{00}| \right) \left(\sup_{\tau} d_{\mathcal{M}}(\gamma(\tau), \mu(\tau)) \right) = O_P \left(h_{\mu}^2 + \sqrt{\frac{\log n}{nmh_{\mu}} + \frac{\log n}{n}} \right)$$

for a universal constant $c > 0$ depending only on \mathcal{K} .

The uniform convergence rates of $R_{00,2} - \partial_s \mathcal{C}(s, t)h_C S_{10} - \partial_t \mathcal{C}(s, t)h_C S_{01}$ and other similar terms are obtained by the same arguments as in Theorem 5.2 of Zhang and Wang (2016), except that no truncation argument is needed due to Assumption 4.1(b). \square

References

- Afsari, B. (2011). Riemannian L^p center of mass: Existence, uniqueness, and convexity. *Proceedings of the American Mathematical Society*, 139(2):655–673.
- Aneiros, G., Cao, R., Fraiman, R., Genest, C., and Vieu, P. (2019). Recent advances in functional data analysis and high-dimensional statistics. *Journal of Multivariate Analysis*, 170:3–9.
- Arsigny, V., Fillard, P., Pennec, X., and Ayache, N. (2006). Log-Euclidean metrics for fast and simple calculus on diffusion tensors. *Magnetic Resonance in Medicine*, 56(2):411–421.
- Arsigny, V., Fillard, P., Pennec, X., and Ayache, N. (2007). Geometric means in a novel vector space structure on symmetric positive-definite matrices. *SIAM Journal of Matrix Analysis and Applications*, 29(1):328–347.
- Bhattacharya, R. and Patrangenaru, V. (2003). Large sample theory of intrinsic and extrinsic sample means on manifolds. I. *The Annals of Statistics*, 31(1):1–29.
- Bhattacharya, R. and Patrangenaru, V. (2005). Large sample theory of intrinsic and extrinsic sample means on manifolds. II. *The Annals of Statistics*, 33(3):1225–1259.
- Cornea, E., Zhu, H., Kim, P., and Ibrahim, J. G. (2017). Regression models on Riemannian symmetric spaces. *Journal of the Royal Statistical Society: Series B (Statistical Methodology)*, 79(2):463–482.
- Dai, X., Lin, Z., and Müller, H.-G. (2020+). Modeling longitudinal data on riemannian manifolds. *Biometrics*, page to appear.
- Dai, X. and Müller, H.-G. (2018). Principal component analysis for functional data on Riemannian manifolds and spheres. *Annals of Statistics*, 46:3334–3361.

- Dryden, I. L., Koloydenko, A., and Zhou, D. (2009). Non-Euclidean statistics for covariance matrices, with applications to diffusion tensor imaging. *The Annals of Applied Statistics*, 3(3):1102–1123.
- Dubey, P. and Müller, H.-G. (2020). Functional models for time-varying random objects. *Journal of the Royal Statistical Society: Series B (Statistical Methodology)*, 82(2):275?–327.
- Faraway, J. J. (2014). Regression for non-Euclidean data using distance matrices. *Journal of Applied Statistics*, 41(11):2342–2357.
- Ferraty, F. and Vieu, P. (2006). *Nonparametric Functional Data Analysis: Theory and Practice*. Springer-Verlag, New York.
- Fillard, P., Arsigny, V., Ayache, N., and Pennec, X. (2005). A Riemannian framework for the processing of tensor-valued images. In *International Workshop on Deep Structure, Singularities, and Computer Vision*, pages 112–123.
- Fletcher, P. T. (2013). Geodesic regression and the theory of least squares on riemannian manifolds. *International journal of computer vision*, 105(2):171–185.
- Fletcher, T. and Joshi, S. (2007). Riemannian geometry for the statistical analysis of diffusion tensor data. *Signal Processing*, 87:250–262.
- Hein, M. (2009). Robust nonparametric regression with metric-space valued output. In *Advances in Neural Information Processing Systems*, pages 718–726.
- Hinkle, J., Fletcher, P. T., and Joshi, S. (2014). Intrinsic polynomials for regression on Riemannian manifolds. *Journal of Mathematical Imaging and Vision*, 50(1-2):32–52.
- Hsing, T. and Eubank, R. (2015). *Theoretical foundations of functional data analysis, with an introduction to linear operators*. John Wiley & Sons.
- Kokoszka, P. and Reimherr, M. (2017). *Introduction to Functional Data Analysis*. Chapman and Hall/CRC.
- Lee, J. M. (1997). *Riemannian Manifolds: An Introduction to Curvature*. Springer-Verlag, New York.
- Lee, J. M. (2002). *Introduction to Smooth Manifolds*. Springer, New York.
- Lenglet, C., Rousson, M., Deriche, R., and Faugeras, O. (2006). Statistics on the manifold of multivariate normal distributions: Theory and application to diffusion tensor MRI processing. *Journal of Mathematical Imaging and Vision*, 25(3):423–444.
- Li, Y. and Hsing, T. (2010). Uniform convergence rates for nonparametric regression and principal component analysis in functional/longitudinal data. *The Annals of Statistics*, 38(6):3321–3351.
- Lin, Z. (2019). Riemannian geometry of symmetric positive definite matrices via cholesky decomposition. *SIAM Journal on Matrix Analysis and Applications*, 40(4):1353–1370.
- Lin, Z. and Müller, H.-G. (2019). Total variation regularized Fréchet regression for metric-space valued data. *arxiv*.
- Lin, Z. and Yao, F. (2019). Intrinsic Riemannian functional data analysis. *The Annals of Statistics*, 47(6):3533–3577.
- Lindberg, O., Walterfang, M., Looi, J. C., Malykhin, N., Östberg, P., Zandbelt, B., Styner, M., Velakoulis, D., Örndahl, E., Cavallin, L., and Wahlund, L.-O. (2012). Shape analysis of the hippocampus in alzheimer’s disease and subtypes of frontotemporal lobar degeneration. *Journal of Alzheimer’s Disease*, 30(2):355–365.
- Moakher, M. (2005). A differential geometry approach to the geometric mean of symmetric positive-definite matrices. *SIAM Journal on Matrix Analysis and Applications*, 26(3):735–747.
- Nichols, David, A., Vines, and Justin (2016). Properties of an affine transport equation and its holonomy. *General Relativity and Gravitation*, 48(127).

- Pelletier, B. (2006). Non-parametric regression estimation on closed Riemannian manifolds. *Journal of Nonparametric Statistics*, 18(1):57–67.
- Pennec, X. (2019). Curvature effects on the empirical mean in riemannian and affine manifolds: a non-asymptotic high concentration expansion in the small-sample regime. *arxiv*.
- Pennec, X. (2020). Manifold-valued image processing with spd matrices. In *Riemannian Geometric Statistics in Medical Image Analysis*, pages 75–134. Elsevier.
- Pennec, X., Fillard, P., and Ayache, N. (2006). A Riemannian framework for tensor computing. *International Journal of Computer Vision*, 66(1):41–66.
- Petersen, A. and Müller, H.-G. (2019). Fréchet regression for random objects with Euclidean predictors. *The Annals of Statistics*, 47(2):691–719.
- Prévôt, C. and Röckner, M. (2007). *A Concise Course on Stochastic Partial Differential Equations*. Springer.
- Ramsay, J. O. and Silverman, B. W. (2005). *Functional Data Analysis*. Springer Series in Statistics. Springer, New York, 2nd edition.
- Rodrigues, W. A. and Capelas de Oliveira, E. (2016). *The Many Faces of Maxwell, Dirac and Einstein Equations*. Springer.
- Schötz, C. (2019). Convergence rates for the generalized Fréchet mean via the quadruple inequality. *arxiv*.
- Shi, X., Styner, M., Lieberman, J., Ibrahim, J. G., Lin, W., and Zhu, H. (2009). Intrinsic regression models for manifold-valued data. In *Medical Image Computing and Computer-Assisted Intervention - MICCAI*, volume 12, pages 192–199.
- Steinke, F., Hein, M., and Schölkopf, B. (2010). Nonparametric regression between general Riemannian manifolds. *SIAM Journal on Imaging Sciences*, 3(3):527–563.
- Sturm, K.-T. (2003). Probability measures on metric spaces of nonpositive curvature. In *Heat kernels and analysis on manifolds, graphs, and metric spaces (Paris, 2002)*, vol. 338 of *Contemporary Mathematics*, pages 357–390. American Mathematical Society, Providence, RI.
- Su, J., Kurtek, S., Klassen, E., and Srivastava, A. (2014). Statistical analysis of trajectories on riemannian manifolds: bird migration, hurricane tracking and video surveillance. *The Annals of Applied Statistics*, 8(1):530–552.
- van der Vaart, A. and Wellner, J. (1996). *Weak Convergence and Empirical Processes: With Applications to Statistics*. Springer, New York.
- Wang, J.-L., Chiou, J.-M., and Müller, H.-G. (2016). Review of functional data analysis. *Annual Review of Statistics and Its Application*, 3:257–295.
- Yao, F., Müller, H.-G., and Wang, J.-L. (2005). Functional data analysis for sparse longitudinal data. *Journal of the American Statistical Association*, 100(470):577–590.
- Zhang, X. and Wang, J. L. (2016). From sparse to dense functional data and beyond. *The Annals of Statistics*, 44:2281–2321.
- Zhang, X. and Wang, J. L. (2018). Optimal weighting schemes for longitudinal and functional data. *Statistics and Probability Letters*, 138:165–170.
- Zhang, Z., Klassen, E., and Srivastava, A. (2018). Phase-amplitude separation and modeling of spherical trajectories. *Journal of Computational and Graphical Statistics*, 27(1):85–97.
- Zhu, H., Chen, Y., Ibrahim, J. G., Li, Y., Hall, C., and Lin, W. (2009). Intrinsic regression models for positive-definite matrices with applications to diffusion tensor imaging. *Journal of the American Statistical Association*, 104(487):1203–1212.